1963

Motion of fluid in a moving vessel

Orest Cochkanoff
Iowa State University

MOTION OF FLUID IN A MOVING VESSEL

by

Orest Cochkanoff

A Dissertation Submitted to the

Graduate Faculty in Partial Fulfillment of

The Requirements for the Degree of

DOCTOR OF PHILOSOPHY

Major Subject: Theoretical and Applied Mechanics

Approved:

Signature was redacted for privacy.

In Charge of Major Work

Signature was redacted for privacy.

Head of Major Department

Signature was redacted for privacy.

Dean of Graduate College

Iowa State University
Of Science and Technology
Ames, Iowa

1963

TABLE OF CONTENTS

INTRODUCTION

A container, partially filled with liquid and subjected to motion, forms the basis for many interesting problems. The most common situation is for the liquid to behave as one interconnected mass, possessing an infinite number of degrees of freedom. The oscillation of such a liquid mass in a vessel is commonly known as "sloshing". If the motion is very vigorous and accelerations greater than gravity exist, the fluid may splash and separate. Such problems have received little attention and would be extremely difficult to solve analytically.

Sloshing problems in engineering first occurred in the design and operation of ships with large ballast and fresh water tanks. When fuel oil came into use the problem was well known although no formal analysis was employed in obtaining solutions. A more recent similar problem is the design of swimming pools for passenger ships.

Another sloshing problem is the design of a dam to withstand earthquake loads. The situation here is essentially that of a moving container filled with liquid.

In the case of aircraft, concern was first expressed about forces due to fuel motion in tip tanks. Some airplanes with large wing tanks had certain flight characteristics affected to a pronounced degree by fuel oscillations. Current, high speed aircraft with thin wings and large fuselage tanks, may develop large sloshing forces during flight. Schy (37) points out that small-amplitude, lightly damped lateral oscillations traced to fuel oscillations are a troublesome characteristic of certain high-speed airplanes. A report by Luskin and Lapin (21)

describes flight experience with aircraft in which fuel sloshing is present to a measured degree. The effect is recorded as a pulsing or time derivative of acceleration in the flight direction. In general, both lateral and longitudinal oscillations of the aircraft can be induced, with corresponding need for trim changes or damping devices.

Most current work on the subject of sloshing deals with the problem of liquid propellants in rockets. At launch, more than 90 percent of the total weight of a rocket consists of the propellants. Any oscillation of this liquid can have a profound effect on flight stability and control, especially if this motion is coupled with the control system. The forces and moments that are produced cause perturbations in the flight path and may cause loss of control with tumbling and break-up of the vehicle. Problems of this type are mentioned by Abramson (1), Bauer (5, 6), Eulitz (11), and Stofan and Sumner (39).

Most of the theoretical work to date has been done in connection with applications to dams or rockets. For the case of dams, the problems that have been studied dealt with rectangular containers moving horizontally or with one wall moving horizontally. For rocket applications, the containers are generally cylindrical with a rather large depth to diameter ratio, but subjected to various motions. Very little experimental work has been done to prove the validity of the assumptions used to linearize the equations, and to check final results. This point is made by Miles (24, 25) and Lawrence et al. (20). The latter paper also points out that some fuel measuring systems use differential pressure pickups. Thus the dynamic effect of the remaining fuel must be known if

proper interpretation of readings is to be expected.

Gleghorn (12) states that more experimental results are required to verify completely the assumptions used for dimensional analysis applied to smooth-walled tanks.

The solution to problems arising from sloshing have been found empirically. In the case of ships, baffles or bulkheads are built in to prevent sloshing and also to add to the structural integrity of the ship. In case of emergency, tanks could also be pumped out or flooded to prevent liquid motion.

For airplanes and rockets, the solution is not so simple because of the weight problem. It is generally agreed that some form of sloshing control is required, otherwise an upper limit must be imposed on tank size. Suitable baffles may be designed only if sloshing behavior is well understood, and even then the approach must still be trial and error.

It is hoped that the study of liquid motion in containers may eventually lead to the development of rational methods of design for such slosh suppression systems.

The problem described herein originated from a suggestion by Pence[x], who indicated the need of a solution for the case of "a horizontal flat container, somewhat less than full, subjected to rotational acceleration about a horizontal axis". The further point was made that some of the equations in use now appear to be in error. Since no experimental results have been reported for sloshing in pitching vessels, the problem was considered to be particularly interesting.

[x]Pence, R. F., Convair, Forth Worth, A Division of General Dynamics Corporation, Forth Worth, Texas. Suggested Thesis Topics. Private communication. May, 1959.

REVIEW OF LITERATURE

The behavior of fluid in a container was first studied by Poisson (31) in 1828 and then Rayleigh (32) in 1876. Horace Lamb (19) published the first extensive treatment of the problem in 1879 in the first edition of his book. This work appears to be the earliest still used in direct reference. The above noted works deal with idealized situations and consider natural oscillations of fluids in vessels filled to either shallow or great depth. Results which are applicable to problems of sloshing, however, were not developed until relatively recently.

The first work on this subject suitable for application to practical problems of sloshing was by Westergaard (45) in 1933. He derived formulas for the water pressure on the vertical upstream face of a straight dam during an earthquake. The analysis was based on motion of the dam face in a horizontal direction perpendicular to its span. Westergaard showed that the dynamic action of the contained water could be simulated by the inertia force of a certain amount of "solidified" water attached to the dam. Hoskins and Jacobsen (15) in 1934 checked Westergaard's theory by an experiment. A rectangular tank was set up on a shaking table and oscillated horizontally. A flexible connector was used as a dynamometer. An elastic impact was supplied by a pendulum which generated a "known" motion. Problems arose due to the inertia of the container and the flexibility of the dynamometer. However, the authors corroborated Westergaard's result that a certain mass of water may be considered fixed to the dam and moving with it while the remainder of the water remains inactive.

The effect of compressibility of water was considered by Werner and Sundquist (44) in 1940. Their analysis dealt with horizontal sinusoidal motion of one wall of the container. In 1949 Jacobsen (17) analyzed the case of impulsive ground displacements in the horizontal direction for the case of an incompressible, inviscid fluid. Gravity waves were not considered in this work. Zangar (47) in 1953 reported on his use of an electrical analogy for such problems, but again the surface boundary condition used did not permit gravity waves. Housner (16) in 1957 presented a simplified analysis for the hydrodynamic pressure developed when a fluid container is subjected to a horizontal acceleration.

The application of sloshing theory to aeronautical problems was developed largely in the early 1950's. In 1941 Smith (38) discussed the probable effect of sloshing on lateral stability of aircraft models. In 1951 Luskin and Lapin (21) and Schy (37) discussed the relation of sloshing modes to aircraft dynamic analysis. Merten and Stephenson (22) investigated the behavior of fluid in a cylindrical horizontal vessel (tip-tank) moving in a direction transverse to the axis, but their work appears to be of little interest since splashing rather than sloshing occurred for the range of values they tested. Widmayer and Reese (46) in 1953 studied the effective moment of inertia of the fluid in tanks undergoing pitching oscillations. In 1955 Reese and Sewall (33) studied the behavior of sloshing fuel in tip-tanks mounted on swept-wings undergoing torsional oscillations.

Most of these studies were based on specific situations or were

generalized to such an extent that numerical calculations for other tanks could not be carried out using these reports.

The forces produced by fuel oscillation in a rectangular tank were discussed by Graham (13) in 1950. Graham introduced the concept of a spring-mass system as an analog to the oscillating fluid. In this approach, the fluid was divided into two parts. One mass was fixed to the tank and the other was spring mounted. The location and magnitude of the masses could be calculated so that the total mass, location of the center of gravity, and the forces would be correct for the model. This paper was further extended by Graham and Rodriguez (14) in 1951 to describe the behavior of a system with translation, pitching and rotation. No experiments were carried out to test the theory developed. A more useful analogy was presented by Kachigan (18) who used a pendulum to represent the oscillating fluid mass.

The above-mentioned analogies are most useful in describing the dynamic action of a complete aircraft and enable a designer to calculate the various modes of oscillation. Luskin and Lapin (21) describe the basic form of stability analysis required for an aircraft when fuel sloshing is present. If only the fundamental fuel sloshing mode is considered and the analysis is simplified by excluding cross-products or uncoupling the system, then it is possible to solve for the three oscillatory modes. These are the phugoid, the short-period motion and the fuel-sloshing mode.

During this same period of time, studies on fluid motion in moving vessels were also carried out by persons interested in the phenomena

per se. Binnie (8) in 1941 presented an approximate theory for the waves formed in oscillating tanks. Penny and Price (27) in 1952 used a rather intuitive approach but reached some interesting conclusions regarding the nature of standing waves. None of these research projects involved any experimental work to check the theory that was developed.

In 1953 G. I. Taylor (43) reported on experiments to test the conclusions arrived at by Penny and Price in their analytical study. Taylor used a tank with opposite sides pivoted so that they moved in and out, in opposition to each other, creating a "bobbing" or symmetrical type of fluid motion. Pictures taken of the wave profiles confirmed the analytical results of Penny and Price.

The development of liquid-propelled rockets influenced the next period of studies of sloshing behavior to such an extent that virtually all current work deals with cylindrical tanks. Kachigan (18) in 1955 presented a solution for the case of such a tank subjected to transverse oscillation. This was followed by Schmitt (35) in 1956 who obtained results for the oscillation of fluid in a cylindrical container undergoing translation and rotation. A correction was published in another paper by Schmitt (36) the following year.

Gleghorn (12) in 1957 reporting on the status of work to date, especially as related to specific designs, mentions the need for some experimental work to verify the theoretical analysis used. The first record of such experiments with results applicable to rocket propellant sloshing was conducted by Bulitz (11) in 1957. A large cylindrical tank was oscillated in a horizontal direction by a crank mechanism. The two

lowest natural frequencies of sloshing were checked experimentally.

Abramson and Ransleben (2, 3) in 1958 to 1960 ran a comprehensive series of model experiments to verify the solutions for cylindrical tanks. Their research was conducted on an elaborate test-rig including a test platform on rollers and another dummy platform moving 180 degrees out of phase to counterbalance inertia forces of all moving parts except the fluid. The facility was designed to permit rotational or pitching inputs, although no such experiments have been conducted as yet. The results recorded for sinusoidal translation of model tanks agrees quite well with the few larger-scale tests made by Eulitz (11). Abramson and Ransleben (2) were the first to apply similitude to the problem and to design their experiments so that their results could apply to the much larger prototypes. They point out that the results of several previous investigators are of limited value because this important step was not taken. Sandorff (34) in 1960 extended the similitude approach to include flexible-wall tanks and also takeoff and unsymmetrical load conditions. This report also deals with similitude considerations for the structural portions of the tank, although such methods are well known, for example, see Murphy (26).

Lawrence et al. (20) employed the variational method to tanks with bottoms that were not flat. In practice, this method is reported of limited use since proper approximate functions must be chosen and this is not easy for complicated shapes.

Recently, (June, 1963), experiments have been reported on toroidal tanks by Summer (42) and spherical tanks by Stofan and Sumner (39).

The problem of flexibility of the container has been discussed by Miles (24) and most recently by Bauer (6). A cylindrical tank is the basis for both test reports.

An interesting recent paper (July, 1963) by Bauer (5) deals with the overall influence of sloshing on the stability boundaries of a typical space booster. Cases of one, two, or three cylindrical or concentric tanks are dealt with. The effect of parameters such as control frequency and damping, and the sloshing mass, its frequency, and location are all considered.

Aeronautical or astronautical application of sloshing analysis invariably leads to the problem of slosh suppression or prevention. It is generally acknowledged that significant damping is obtained only if some form of baffle is used in the system. Baffles usually depend on the viscosity of the fluid for their effectiveness. For this reason and because of the difficult boundary conditions, analysis of fluid action when baffles are present is not easy and no solutions are available. A strictly empirical approach must be used. Often the design consists simply of extending frames or other structural members into the tank. In many reports, for example Schy (37), no mention is made of the reasons for the particular configuration of baffles employed.

The most common form of baffle used in liquid propellant tanks is formed by circular rings inside the tank. Gleghorn (12) reports on the success of such baffles in the Thor missile. Two recent papers which discuss baffle designs of this type were written by Miles (24, 25).

Eulitz (11) has reported on an "egg-crate" system of baffles,

although this type is conceded to have a large weight penalty for long rockets. The principle involved is the formation of a large number of small tanks. Many other papers have been written that deal with the design or selection of baffles for specific vehicles but these do not contribute to a better understanding of the basic problem of sloshing.

Another suppression device that has been used is the float system. Abramson and Ransleben (3) report on a system employing over 90 cans floating on the surface of the fuel in a cylindrical tank to inhibit sloshing. Again the boundary conditions were such as to preclude successful analytical solution and recourse to model study was made.

A recent report by Stofan and Sumner (39) discusses the use of positive-expulsion bags for slosh damping. This diaphragm-type device has been tried on models of spherical containers, but would appear of little value for cylindrical or rectangular vessels.

Baffles are essentially a corrective device for a system which does not behave properly in its original configuration. They add weight and decrease payload for any vehicle in which they are required. Their design is largely an art and is not done according to any defined procedure based on engineering analysis. A preferable solution would be choice of a tank form such that sloshing is suppressed or at least the forces are kept low and the frequency high to avoid problems of instability. Bauer (5) also mentions that a solution to sloshing problems in rockets may be obtained if the type, location and gain of the control sensors are wisely chosen. It is believed that this type of control cannot be relied upon at present.

In any case, if sloshing is to be prevented or if an intuitive approach is to be used for baffle design, it is necessary to have a much better understanding of fluid behavior in a moving vessel. Ultimately more refined methods of sloshing control may be developed.

THEORETICAL ANALYSIS

Basic Theory

Consider a rigid, rectangular tank, partly filled with liquid, as shown in Fig. 1. The origin of an x, y, z coordinate system is located at the center of gravity of the undisturbed liquid mass. The fluid is assumed to be incompressible with density ρ. Surface tension effects may be neglected for vessels of the size involved in most sloshing problems, although a special case involving this property is presented later. Case and Parkinson (9) point out that surface tension may be neglected for oscillation of fluid in cylinders with diameters as small as 3 inches.

The fluid viscosity is also neglected for the analysis. This assumption allows a potential function to be used to obtain a solution. Justification for this assumption appears well-founded. Gleghorn (12) notes that natural viscous damping in a smooth-walled tank is extremely small (in the order of 0.01%), although the basis for this numerical value is not given. Other authors, for example, Luskin and Lapin (21) state that significant damping is obtained only if baffles are used. Abramson and Ransleben (2, 3) in reporting on the most extensive model tests conducted to date, point out that stiffeners of three percent tank diameter extending into the liquid have a minor effect on reducing sloshing motions. Without baffles, viscous effects are said to be negligibly small.

The vessel is assumed either to be moving with a constant acceleration in a vertical path along the z-axis or not translating at all.

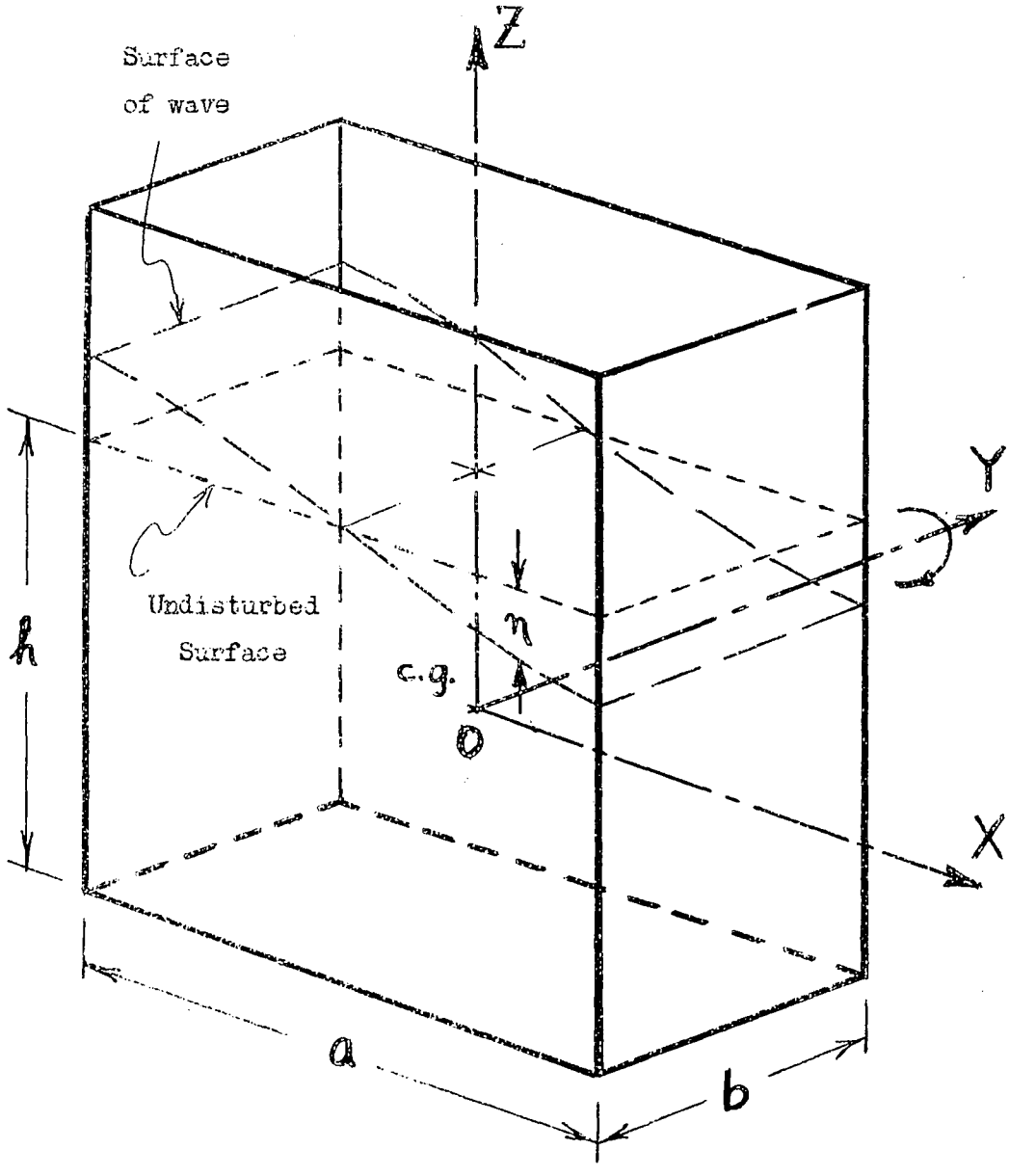

Fig. 1. Coordinate system for rectangular tank

The "effective" acceleration is thus a constant times g and is denoted by γ.

The sloshing is excited by a time-dependent acceleration about the y-axis. The impressed motion is a rotation with frequency ω and with an amplitude β radians. The wave height above the original undisturbed surface is given by η.

The top of the vessel may be closed at any point above the wave crest since tank ullage is not a variable for an incompressible fluid as long as separation does not take place.

In the equations that follow, the notations used are essentially those of Lamb (19).

If at any point x, y, z in the fluid mass, an element has velocities u, v and w at any time, then consideration of continuity of flow for the element at that point results in the equation of continuity

$$\frac{\partial u}{\partial x} + \frac{\partial v}{\partial y} + \frac{\partial w}{\partial z} = 0$$

Since the flow is independent of y, only the two dimensions x and z need be retained. In addition to the above, the fluid must satisfy the conditions imposed by internal friction or viscosity. In the case of an inviscid fluid the condition of irrotational flow applies

$$\frac{\partial w}{\partial x} - \frac{\partial u}{\partial z} = 0$$

and a potential function ϕ exists, such that

$$u = -\frac{\partial \phi}{\partial x}$$

$$w = -\frac{\partial \phi}{\partial z}$$

It is evident that the irrotational flow condition is satisfied with the

above terms. Substitution into the continuity equation gives Laplaces' equation for two-dimensional irrotational flow

$$\frac{\partial^2 \phi}{\partial x^2} + \frac{\partial^2 \phi}{\partial z^2} = 0 \qquad (1)$$

This equation must be solved using the appropriate boundary conditions.

For the free surface, the boundary condition is based on the fact that pressure on this surface is constant and may be taken equal to zero without loss of generality. An element in two-dimensional flow at a point x, z is considered at a time t. The body forces per unit mass at the point are given by X and Z and the pressure at the point is p. Applying Newton's Law results in the equation in the x-direction

$$\rho X - \frac{\partial p}{\partial x} = \rho \frac{Du}{Dt}$$

Substituting

$$\frac{Du}{Dt} = \frac{\partial u}{\partial t} + u \frac{\partial u}{\partial x} + w \frac{\partial w}{\partial z}$$

into the equations for both the x and z-directions, gives Euler's equations

$$\frac{\partial u}{\partial t} + u \frac{\partial u}{\partial x} + w \frac{\partial u}{\partial z} = X - \frac{1}{\rho} \frac{\partial p}{\partial x}$$

$$\frac{\partial w}{\partial t} + u \frac{\partial w}{\partial x} + w \frac{\partial w}{\partial z} = Z - \frac{1}{\rho} \frac{\partial p}{\partial z}$$

If the forces X and Z are conservative they may be defined in terms of a potential Ω, which is the potential energy per unit mass at the point x, z with respect to force at a distance. For the analysis to follow Ω will be taken as a constant with respect to time such that

$$X = -\frac{\partial \Omega}{\partial x} \quad \text{and} \quad Z = -\frac{\partial \Omega}{\partial z}$$

The potential functions ϕ and Ω allow Euler's equations to be written in the form

$$-\frac{\partial^2\phi}{\partial x\,\partial t}+u\frac{\partial u}{\partial x}+w\frac{\partial u}{\partial z}=-\frac{\partial\Omega}{\partial x}-\frac{1}{\rho}\frac{\partial p}{\partial x}$$

$$-\frac{\partial^2\phi}{\partial z\,\partial t}+u\frac{\partial w}{\partial x}+w\frac{\partial w}{\partial z}=-\frac{\partial\Omega}{\partial z}-\frac{1}{\rho}\frac{\partial p}{\partial z}$$

The irrotational flow conditions can now be used to reduce each equation to only one space variable

$$-\frac{\partial^2\phi}{\partial x\,\partial t}+u\frac{\partial u}{\partial x}+w\frac{\partial w}{\partial x}=-\frac{\partial\Omega}{\partial x}-\frac{1}{\rho}\frac{\partial p}{\partial x}$$

$$-\frac{\partial^2\phi}{\partial z\,\partial t}+u\frac{\partial u}{\partial z}+w\frac{\partial w}{\partial z}=-\frac{\partial\Omega}{\partial z}-\frac{1}{\rho}\frac{\partial p}{\partial z}$$

These equations can be integrated with respect to the space variable.

$$-\frac{\partial\phi}{\partial t}+\frac{u^2+v^2}{2}+\Omega+\frac{p}{\rho}=F_1(z,\,t)$$

$$-\frac{\partial\phi}{\partial t}+\frac{u^2+v^2}{2}+\Omega+\frac{p}{\rho}=F_2(x,\,t)$$

It may be seen that $F_1=F_2=F(t)$. Thus, one equation may be written

$$-\frac{\partial\phi}{\partial t}+\frac{u^2+v^2}{2}+\Omega+\frac{p}{\rho}=F(t)$$

The potential $\Omega=\gamma z$ applies to this case since the only body force present is due to the effective acceleration γ. The resulting equation is

$$-\frac{\partial\phi}{\partial t}+\frac{u^2+v^2}{2}+\frac{p}{\rho}+\gamma z=F(t)$$

This is Bernoulli's equation for non-steady flow and relates pressures to velocity changes and fluid level.

The expression for pressure may be written

$$p=\rho\left[\frac{\partial\phi}{\partial t}+F(t)-\frac{u^2+v^2}{2}-\gamma z\right]$$

If the velocities are expressed in terms of the potential function, then a non-linear equation in ϕ is obtained. However, the velocities during sloshing may be assumed small and neglecting the velocity squared terms will linearize the equation without introducing an appreciable error.

Thus $p = \rho\left[\frac{\partial\phi}{\partial t} + F(t) - \gamma z\right]$

For the case of steady motion $\frac{\partial\phi}{\partial t} = 0$ and at the surface $z = \frac{h}{2}$ the pressure may be taken equal to zero.

Thus $F(t) = \frac{\gamma h}{2}$

Using this value of $F(t)$ for the general case

$$p = \rho\left[\frac{\partial\phi}{\partial t} + \gamma\left(\frac{h}{2} - z\right)\right] \tag{2}$$

To establish the boundary condition on the surface, the pressure is taken constant for all time. Thus

$$\frac{Dp}{Dt} = \frac{\partial p}{\partial t} + u\frac{\partial p}{\partial x} + w\frac{\partial p}{\partial z} = 0$$

Substituting for p and performing the differentiations, gives the following equation

$$\rho\left[\frac{\partial^2\phi}{\partial t^2} + u\frac{\partial^2\phi}{\partial x\partial t} + w\frac{\partial^2\phi}{\partial z\partial t} - w\gamma\right] = 0$$

or $$\rho\left[\frac{\partial^2\phi}{\partial t^2} - u\frac{\partial u}{\partial t} - w\frac{\partial w}{\partial t} - w\gamma\right] = 0$$

Since the velocities and their time derivatives can be assumed small, the products in the middle terms may be considered negligible, so that the surface boundary condition is obtained.

$$\frac{\partial^2\phi}{\partial t^2} + \gamma\frac{\partial\phi}{\partial z} = 0 \tag{3}$$

This is true for the liquid surface at an elevation $z = \frac{h}{2} + \eta$. However, if the wave amplitude is limited to small values, this linearized boundary condition may be assumed to hold for the case $z = \frac{h}{2}$.

The other boundary conditions are kinematic and deal with the direction of the flow at a solid boundary. For sinusoidal pitching about the y-axis, the rotational displacement at any time is given by $\beta \sin \omega t$. For small values of β, the boundary conditions are assumed to apply to the fixed boundaries $x = \pm \frac{a}{2}$ and $z = -\frac{h}{2}$. The surface boundary condition is not affected as long as β is kept small,

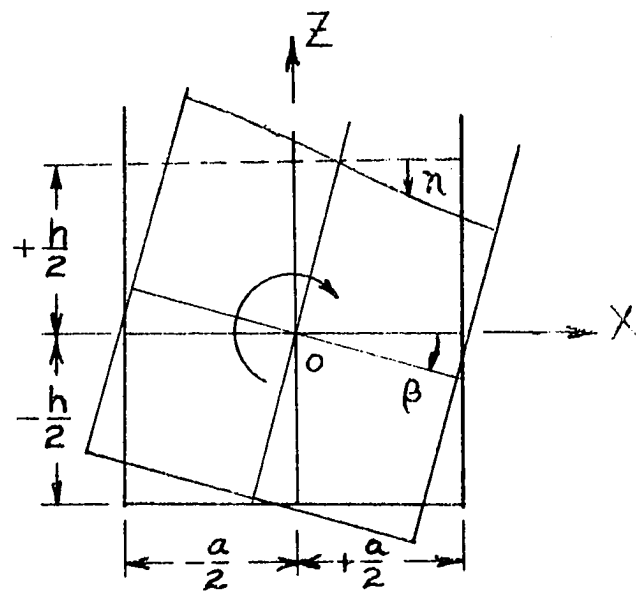

Fig. 2. Boundary conditions for tank.

The boundary condition along the end walls $x = \pm \frac{a}{2}$ is

$$u = -\frac{\partial \phi}{\partial x} = \omega\beta z \cos \omega t \tag{4}$$

and along the bottom at $z = -\frac{h}{2}$

$$w = -\frac{\partial \phi}{\partial z} = -\omega\beta x \cos \omega t. \tag{5}$$

It is of interest to interpret the last two boundary conditions as separate physical motions. Condition (3) may be visualized as an effect produced by the end walls pivoting about their intersection point on the x-axis. Condition (4) may be interpreted as a pivoting of the bottom about the point of intersection with the z-axis.

A solution to the problem may thus be obtained by solving Laplace's equation and satisfying the linearized free surface condition and the moving wall conditions. The boundary conditions introduce time and so the result is a time-dependent or non-steady solution.

Solution of Equations

The time-dependent boundary conditions are not easily applied to the solution of field problems. A convenient change of variable can be found by letting

$$F = \frac{\phi}{\cos \omega t}$$

Thus the Laplace equation (1) becomes

$$\left(\frac{\partial^2 F}{\partial x^2} + \frac{\partial^2 F}{\partial z^2} \right) \cos \omega t = 0$$

Since this is satisfied at all values of t, the new Laplace equation is

$$\frac{\partial^2 F}{\partial x^2} + \frac{\partial^2 F}{\partial z^2} = 0 \tag{6}$$

The surface boundary condition for $z = \frac{h}{2}$ becomes

$$\gamma \frac{\partial F}{\partial z} - \omega^2 F = 0 \tag{7}$$

The boundary condition along the end walls $x = \pm \frac{a}{2}$ is now

$$\frac{\partial F}{\partial x} = - \omega \beta z \tag{8}$$

Along the bottom of the tank, for $z = - \frac{h}{2}$

$$\frac{\partial F}{\partial z} = \omega \beta x \tag{9}$$

The equations are now expressed in terms of the variables x, z with t not directly included.

In order to proceed to a solution for the case where more than one boundary condition is nonhomogeneous, it is convenient to assume a solution in parts. That is, a solution of the form $F = F_1 + F_2$ is taken.

For the case of F_1, the boundary condition (8) for $x = \pm \frac{a}{2}$ is taken to be homogeneous

$$\frac{\partial F_1}{\partial x} = 0 \tag{10}$$

The other boundary conditions remain as before. This means that the end walls are now considered stationary while the other conditions are unchanged.

A solution of the form $F_1 = X(x)Z(z)$ is now assumed. If the variables can be separated as this implies, then substitution in the Laplace equation gives

$$\frac{X''}{X} = - \frac{Z''}{Z} = \pm k^2$$

Using the negative value of k^2 will give the two equations

$$X'' + k^2 X = 0$$

$$Z'' - k^2 Z = 0$$

The solutions can be expressed in the form

$$Z = (A_1 \cosh kz + B_1 \sinh kz) \tag{11}$$

$$\text{and } X = (C_1 \cos kx + D_1 \sin kx) \tag{12}$$

The solution F_1 is formed by the product of these with the appropriate values of the constants.

If boundary condition (10) is now applied, the constant C_1 is found to equal zero. This is expected, since a pitching motion of the vessel would not produce an even or "bobbing" form of sloshing. The constant D_1 can be incorporated into A_1 and B_1, and the solution for F_1 now is

$$F_1 = (A_1 \cosh kz + B_1 \sinh kz) \sin kx \tag{13}$$

The condition for $x = \pm \frac{a}{2}$ may be applied again to obtain values of k

$$k = \frac{\pi}{a}(2n-1) \qquad \text{for } n = 1, 2, 3, \ldots \tag{14}$$

It can be shown that the case $k = 0$ leads to a trivial solution.

Boundary condition (9) can now be applied.

$$\frac{\partial F_1}{\partial z} = A_1 \frac{\pi}{a}(2n-1) \sinh\left[\pi(2n-1)\frac{z}{a}\right] + B_1 \frac{\pi}{a}(2n-1) \cosh\left[\pi(2n-1)\frac{z}{a}\right] \sin\left[\pi(2n-1)\frac{x}{a}\right]$$

For the case $z = -\frac{h}{2}$ the sum of all such terms must converge to $\omega\beta x$. Assuming this is so

$$\sum_{n=1}^{\infty} \left\{ -A_n \frac{\pi}{a}(2n-1) \sinh\left[\frac{\pi}{2}(2n-1)\frac{h}{a}\right] + B_n \frac{\pi}{a}(2n-1) \cosh\left[\frac{\pi}{2}(2n-1)\frac{h}{a}\right] \sin\left[\pi(2n-1)\frac{x}{a}\right] \right\} = \omega\beta x \tag{15}$$

This can also be expressed in the form below if a Fourier series expansion is used.

$$\sum_{n=1}^{\infty} b_n \sin\left[\pi(2n-1)\frac{x}{a}\right] = \omega\beta x = f(x)$$

where b_n is the Fourier coefficient

$$b_n = \frac{2}{a}\int_{-\frac{a}{2}}^{+\frac{a}{2}} f(x) \sin\left[\pi(2n-1)\frac{x}{a}\right] dx$$

$$b_n = \frac{2\omega\beta}{a}\left[\frac{a^2}{\pi^2(2n-1)^2}\left\{\sin\left[\pi(2n-1)\frac{x}{a}\right] - \pi(2n-1)\frac{x}{a}\cos\left[\pi(2n-1)\frac{x}{a}\right]\right\}\right]_{-\frac{a}{2}}^{+\frac{a}{2}}$$

Thus $b_n = \frac{-4\omega\beta a}{\pi^2}\frac{(-1)^n}{(2n-1)^2}$

This value can be equated to the constant term in equation (15) to obtain one equation relating A_n and B_n.

$$A_n \sinh\left[\frac{\pi}{2}(2n-1)\frac{h}{a}\right] - B_n \cosh\left[\frac{\pi}{2}(2n-1)\frac{h}{a}\right] = \frac{4\omega\beta a^2}{\pi^3}\frac{(-1)^n}{(2n-1)^3} \qquad (16)$$

Another expression for these constants can be found from the surface boundary condition applied to F_1 to give the equation below.

$$A_n\left\{\frac{\pi}{a}(2n-1)\sinh\left[\frac{\pi}{2}(2n-1)\frac{h}{a}\right] - \omega^2\cosh\left[\frac{\pi}{2}(2n-1)\frac{h}{a}\right]\right\}$$
$$+ B_n\left\{\frac{\pi}{a}(2n-1)\cosh\left[\frac{\pi}{2}(2n-1)\frac{h}{a}\right] - \omega^2\sinh\left[\frac{\pi}{2}(2n-1)\frac{h}{a}\right]\right\} = 0 \qquad (17)$$

The values A_n and B_n can be found by the simultaneous solution of these equations. The first part of the solution is then found by substituting for k in equation (13) and using the appropriate values of A_n and B_n as determined by the preceding analysis. Thus

$$F_1 = \sum_{n=1}^{\infty} \left\{ A_n \cosh\left[\pi(2n-1)\frac{z}{a}\right] + B_n \sinh\left[\pi(2n-1)\frac{z}{a}\right] \right\} \sin\left[\pi(2n-1)\frac{x}{a}\right] \qquad (18)$$

where

$$A_n = \frac{4\omega\beta a^2(-1)^n}{\pi^3(2n-1)^3} \frac{\left\{\frac{\pi}{a}(2n-1)\cosh\left[\frac{\pi}{2}(2n-1)\frac{h}{a}\right] - \omega^2 \sinh\left[\frac{\pi}{2}(2n-1)\frac{h}{a}\right]\right\}}{\left\{\frac{\pi}{a}(2n-1)\sinh\left[\pi(2n-1)\frac{h}{a}\right] - \omega^2\cosh\left[\pi(2n-1)\frac{h}{a}\right]\right\}} \qquad (19)$$

and

$$B_n = \frac{-4\omega\beta a^2(-1)^n}{\pi^3(2n-1)^3} \frac{\left\{\frac{\pi}{a}(2n-1)\sinh\left[\frac{\pi}{2}(2n-1)\frac{h}{a}\right] - \omega^2\cosh\left[\frac{\pi}{2}(2n-1)\frac{h}{a}\right]\right\}}{\left\{\frac{\pi}{a}(2n-1)\sinh\left[\pi(2n-1)\frac{h}{a}\right] - \omega^2\cosh\left[\pi(2n-1)\frac{h}{a}\right]\right\}} \qquad (20)$$

provided the denominator does not vanish.

The solution for F_2 can also be assumed to be a product of the form $F_2 = XZ$ where $Z = (A_2 \cos kz + B_2 \sin kz)$

and $X = (C_2 \sinh kx + D_2 \cosh kx)$

The free surface boundary condition still applies. The boundary condition for the ends of the tank, equation (8) is now retained as a non-homogeneous condition, while the condition for the bottom is made homogeneous. Thus equation (9) for $z = -h/2$ is changed to

$$\frac{\partial F}{\partial z} = 0 \qquad (21)$$

This last condition is now applied to the assumed solution and the relation below is obtained.

$$B_2 = -A_2 \tan\frac{kh}{2}$$

If this is substituted into the assumed solution and the constant A_2 incorporated into C_2 and D_2 the resulting equation is

$$F_2 = (\cos kz - \tan\frac{kh}{2}\sin kz)(C_2 \sinh kx + D_2 \cosh kx) \qquad (22)$$

The boundary condition for the free surface can now be applied to give

$$-2\gamma k \tan\frac{kh}{2} - \omega^2 + \omega^2 \tan^2\frac{kh}{2} = 0$$

This quadratic in $\tan \frac{kh}{2}$ can be solved to give

$$\tan kh = -\frac{\omega^2}{k\gamma}$$

A more convenient form is obtained by using the reciprocal form

$$\operatorname{ctn} kh = -\frac{k\gamma}{\omega^2}$$

The value kh is required on the right side

$$\operatorname{ctn} kh = -\frac{\gamma\,(kh)}{\omega^2 h} \tag{23}$$

This implicit equation in kh can be solved either graphically or by use of tables. An infinite number of discrete values for kh result for any particular choice of γ, ω, and h. The discrete values of k so obtained are denoted k_n.

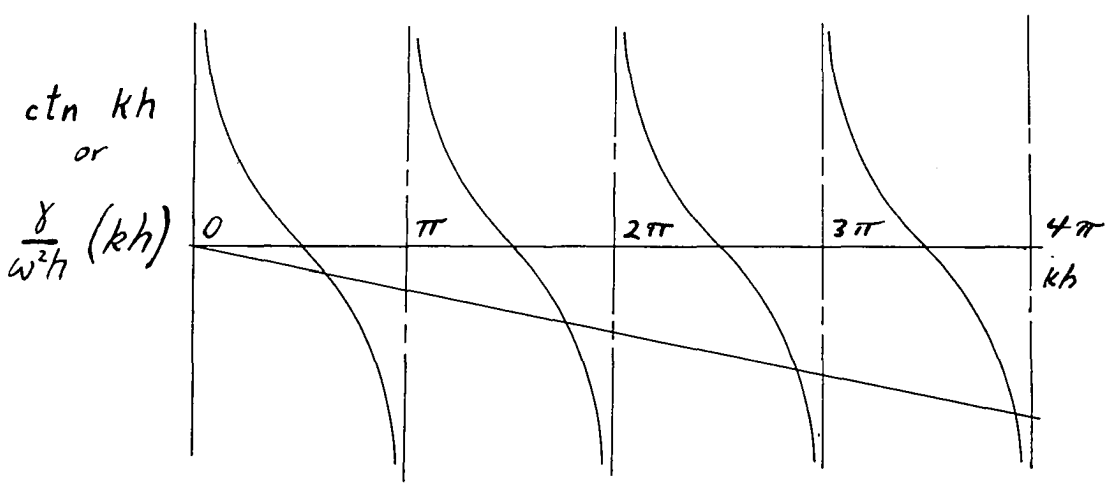

Fig. 3. Graphical solution for k_n.

Boundary condition (8) for the end walls is now applied.

$$\frac{\partial F_2}{\partial x} = k(\cos kz - \tan \frac{kh}{2} \sin kz)\,(C_2 \cosh kx + D_2 \sinh kx)$$

When $x = \pm \frac{a}{2}$, this value $= -\omega\beta z$ and thus D_2 must equal zero. The only

remaining constant now is C_2. The double boundary condition for $x = \pm \frac{a}{2}$ is applied further and a series of terms is now used.

$$\sum_{n=1}^{\infty} C_{2n} k_n \left(\cos k_n z - \tan \frac{k_n h}{2} \sin k_n z\right) \cosh \frac{k_n a}{2} = - \omega\beta z$$

The portion in the brackets consists of a sine and a cosine term and can be interpreted to be equivalent to a cosine function with a phase angle.

$$\sqrt{\tan^2 \frac{k_n h}{2} + 1} \quad \cos\left[\frac{k_n h}{2} \left(\frac{2z}{h} + 1\right)\right]$$

With this substitution the previous equation becomes

$$\sum_{n=1}^{\infty} C_{2n} k_n \sqrt{\tan^2 \frac{k_n h}{2} + 1} \quad \cosh \frac{k_n a}{2} \quad \cos\left[k_n h \left(\frac{z}{h} + \frac{1}{2}\right)\right] = - \omega\beta z \quad (24)$$

But it is also possible to express the right hand side in terms of a Fourier Series.

$$\sum_{n=1}^{\infty} b_n \cos\left[k_n h \left(\frac{z}{h} + \frac{1}{2}\right)\right] = - \omega\beta z \quad (25)$$

From the fundamental properties of Fourier coefficients as given by Churchill (10) the value of b_n may be found from the equation below.

$$\int_{-\frac{h}{2}}^{+\frac{h}{2}} (- \omega\beta z) \cos\left[k_n h \left(\frac{z}{h} + \frac{1}{2}\right)\right] dz = b_n \int_{-\frac{h}{2}}^{+\frac{h}{2}} \cos^2\left[k_n h \left(\frac{z}{h} + \frac{1}{2}\right)\right] dz \quad (26)$$

The value found for b_n from the above is

$$b_n = \frac{-2\omega\beta \left[\cos (k_n h) - 1 + \frac{k_n h}{2} \sin k_n h\right]}{k_n^2 \left[h + \frac{\sin 2 k_n h}{2k_n}\right]}$$

Examination of equations (24) and (25) shows that the value of C_{2n} may be expressed in terms of b_n.

$$C_{2n} = \frac{b_n}{k_n \sqrt{\tan^2\left(\frac{k_n h}{2}\right) + 1} \cosh \frac{ka}{2}}$$

When the value of b_n is substituted in this equation, the value of C_{2n} is found to be.

$$C_{2n} = \frac{-2\omega\beta \left[\cos(k_n h) - 1 + \frac{k_n h}{2} \sin(k_n h)\right]}{k_n^2 \left(k_n h + \frac{1}{2} \sin 2k_n h\right) \sqrt{\tan^2\left(\frac{k_n h}{2}\right) + 1} \cosh \frac{k_n a}{2}}$$

This value is now substituted into the assumed value of F_2 from equation (22). The latter equation is first rewritten using the values found for the various terms as indicated in the preceding analysis:

$$F_2 = \sum_{n=1}^{\infty} C_{2n} \sqrt{\tan^2\left(\frac{k_n h}{2}\right) + 1} \cos\left[k_n h \left(\frac{z}{h} + \frac{1}{2}\right)\right] \sinh k_n x$$

It is convenient to incorporate all the constants into one term. Thus, the final solution is expressed in the following equation.

$$F_2 = \sum_{n=1}^{\infty} C_n \cos k_n h \left(\frac{z}{h} + \frac{1}{2}\right) \sinh (k_n x) \tag{27}$$

where

$$C_n = \frac{-2\omega\beta \left[\cos(k_n h) - 1 + \frac{k_n h}{2} \sin(k_n h)\right]}{k_n^2 \left[k_n h + \frac{1}{2} \sin 2k_n h \right] \cosh\left(\frac{k_n h}{2} \frac{a}{h}\right)} \tag{28}$$

The complete solution to the problem consists of $\phi = F \cos \omega t$ or

$$\phi = (F_1 + F_2) \cos \omega t \tag{29}$$

where F_1 is given by equation (17) and F_2 by equation (27).

Natural Frequencies

The natural frequencies or modes ω_n may be found by determining the values of ω for which the amplitude tends to infinity. At such frequencies, the velocities also tend to infinity in order for the motion to remain oscillatory. The values of ω for which $\frac{\partial \phi}{\partial z}$ or $\frac{\partial \phi}{\partial x}$ tend to infinity may be found from examination of equations (18) and (27) and the equations for the constants used in these solutions. It is seen that the motion tends to infinity when the denominator terms are equated to zero. Proceeding in this manner, the natural frequency is found to be

$$\omega_n^2 = \gamma \frac{\pi}{a} (2n-1) \tanh \left[\pi(2n-1)\frac{h}{a}\right] \quad \text{for } n = 1, 2, 3, \ldots \qquad (30)$$

The preceding equation is found from the denominator of F_1. A similar analysis of the denominator for F_2 does not add any more significant modes.

Equation for Surface

The equation for the liquid surface can be found from equation (2) which gives the pressure in terms of the potential function. The elevation of the surface is given by $z = \frac{h}{2} + \eta$ (refer to Fig. 1). If the pressure at the surface is taken equal to zero, then substitution into equation (2) gives

$$0 = \rho\left[\frac{\partial \phi}{\partial t} + \gamma \left(\frac{h}{2} - z\right)\right]_{z = \frac{h}{2} + \eta}$$

thus $$\frac{h}{2} - z = -\frac{1}{\gamma}\left(\frac{\partial \phi}{\partial t}\right)\Bigg|_{z = \frac{h}{2} + \eta}$$

$$\eta = \frac{1}{g} \left(\frac{\partial \phi}{\partial t}\right)_{z = \frac{h}{2} + \eta}$$

Since η is to be solved for, the value $\frac{h}{2} + \eta$ can not be substituted into the equation. However, if small amplitude motion is assumed, then $z = \frac{h}{2}$ will result in small error and should give a good approximation to the surface shape.

Thus the equation for the surface is taken to be

$$\eta = \frac{1}{g} \left(\frac{\partial \phi}{\partial t}\right)_{z = \frac{h}{2}} \tag{31}$$

But from equation (29) the value of $\frac{\partial \phi}{\partial t}$ can be found to be

$$\frac{\partial \phi}{\partial t} = \frac{\partial}{\partial t} (F_1 + F_2) \cos \omega t$$

or $$\frac{\partial \phi}{\partial t} = - \omega (F_1 + F_2) \sin \omega t$$

Substituting this into equation (31) for the surface shape gives

$$\eta = - \frac{\omega}{g} (F_1 + F_2) \sin \omega t \Big|_{z = \frac{h}{2}}$$

The maximum displacement or amplitude is denoted by η_o and is

$$\eta_o = - \frac{\omega}{g} (F_1 + F_2) \Big|_{z = \frac{h}{2}} \tag{32}$$

Pressure Along Boundaries

The pressure along the tank surfaces may also be found by using equation (2) which is repeated below.

$$p = \rho \left[\frac{\partial \phi}{\partial t} + g \left(\frac{h}{2} - z\right) \right] \tag{2}$$

In this expression the static pressure is given by $p_s = \rho \gamma \left(\frac{h}{2} - z\right)$ which assumes a zero surface pressure. The dynamic pressure is given by $p_d = \rho \frac{\partial \phi}{\partial t}$ where ϕ is the value $(F_1 + F_2) \cos \omega t$.

Thus

$$p_d = - \rho\omega (F_1 + F_2) \sin \omega t \tag{33}$$

By the use of this equation, it is possible to find the pressure along the sides and bottom of the tank.

APPLICATION OF SIMILITUDE TO SLOSHING

Basic Analysis

It is of some interest to examine sloshing from a similitude point of view because many sloshing problems of interest to spacecraft designers are encountered under conditions of either low or high g loadings, while laboratory experiments are generally conducted under one g conditions. A knowledge of similitude is necessary to properly interpret test results for such design conditions. The method used in this analysis follows the procedure outlined by Murphy (26).

The variables that enter into the problem are listed in Table 1. Certain other quantities listed below are not considered in the analysis for the reasons given.

Compressibility This effect is neglected since sloshing is a "low frequency" phenomenon and shock or pressure waves are not of prime importance. Also pressure changes are small and the volume of liquid is essentially constant.

Vapor pressure This variable is neglected since cavitation, gas entrainment and similar problems are not of prime interest in this investigation.

Temperature Although temperature is not a prime variable, it appears indirectly since values of viscosity, density, and surface tension depend on it. Thus temperature must be held constant for each system at the value used for determination of these properties.

Flexibility of Vessel The tank is assumed rigid. This is a reasonable assumption for many applications but may not be legitimate for

aircraft or spacecraft applications. In any case the stiffness of the tank walls could be simulated readily for any particular application. A discussion of structural similitude is given by Murphy (26) and an application to a tank in a spacecraft is made by Sandorff (34).

Table 1. Variables involved in sloshing

No.	Variable	Description	Dimension
1	a	Tank length	L
2	h	Undisturbed liquid height	L
3	l	Any length	L
4	ω	Disturbing frequency	$1/T$
5	t	Any time	T
6	β	Amplitude of disturbance	----
7	ρ	Density of liquid	M/L^3
8	μ	Viscosity of liquid	M/LT
9	p	Any pressure	M/LT^2
10	γ	Effective acceleration	L/T^2
11	σ	Surface tension	M/T^2

The number of variables that is used is thus eleven. Since three dimensions are involved, the number of Pi terms must be eight according to Buckingham's Theorem. These dimensionless, independent parameters are chosen in such a way that certain well-known groups appear. For

this problem, the eight listed in Table 2 were considered most convenient.

In order for a model to simulate the prototype, it is necessary for the corresponding Pi terms in the two systems to be equal, although this condition is often relaxed somewhat. In the analysis that follows, the subscript p refers to prototype while the subscript m refers to the model.

Table 2. Pi Terms

No.	Pi term	Name
1	h/a	Geometrical ratio
2	l/a	Geometrical ratio
3	ωt	Dimensionless frequency
4	β	Angle
5	$a\omega^2/\gamma$	Froude number
6	$p/\rho a^2\omega^2$	Euler number
7	$a^2\omega\rho/\mu$	Reynolds number
8	$\rho a^3\omega^2/\sigma$	Weber number

From the first Pi term the relationship below is obtained.

$$\frac{h_m}{a_m} = \frac{h_p}{a_p} \tag{34}$$

Thus the length scale may be defined as

$$N_L = \frac{h_p}{h_m} = \frac{a_p}{a_m} \tag{35}$$

In this case and for all other scales, the ratio of prototype variable over model variable is used to define the scale whenever possible.

The second Pi term does not add any new scale, but simply generalizes the use of the length scale.

From the third Pi term, it is possible to obtain a time scale.

$$N_T = \frac{t_p}{t_m} = \frac{\omega_m}{\omega_p} \tag{36}$$

This equation also relates frequencies for the two systems.

The Pi terms consisting of angles, show that angles must be preserved and can not be distorted. This condition has already been fulfilled by the constant length scale, which ensures geometrical similarity.

The Pi term containing $\frac{a\omega^2}{\gamma}$ relates the effect of gravity or system acceleration to the dynamic action of the fluid and is known as Froude number. By equating model to prototype Froude numbers, an acceleration scale is obtained.

$$N_g = \frac{\gamma_p}{\gamma_m} = \frac{a_p}{a_m} \frac{\omega_p^2}{\omega_m^2} = \frac{N_L}{N_T^2} \tag{37}$$

The value N_g or the ratio of accelerations, is commonly referred to as the "g" loading.

Equating the Euler numbers, which relate pressures to velocities, will allow a pressure scale to be determined.

$$\frac{p_p}{p_m} = \frac{\rho_p}{\rho_m} \frac{a_p^2}{a_m^2} \frac{\omega_p^2}{\omega_m^2}$$

The density ratio is defined as N_ρ

$$N_\rho = \frac{\rho_p}{\rho_m} \tag{38}$$

Thus

$$N_P = \frac{N_\rho N_L^2}{N_T^2} \tag{39}$$

This equation establishes the pressure ratio for the systems.

The next Pi term is recognized as Reynolds number and is useful in relating inertia forces to viscous forces in the fluid.

$$\frac{a_m^2 \omega_m \rho_m}{\mu_m} = \frac{a_p^2 \omega_p \rho_p}{\mu_p}$$

$$\frac{\mu_p}{\mu_m} = \frac{a_p^2}{a_m^2} \frac{\omega_p}{\omega_m} \frac{\rho_p}{\rho_m}$$

The viscosity ratio is given by N_μ

$$N_\mu = \frac{\mu_p}{\mu_m} \tag{40}$$

Thus

$$N_\mu = \frac{N_L^2}{N_T} N_\rho \tag{41}$$

The final condition brings in the ratio of surface tension to the inertia forces in the fluid and is known as the Weber number. By equating model and prototype Weber numbers the equation below is obtained.

$$\frac{a_p^3}{a_m^3} = \frac{\sigma_p}{\sigma_m} \frac{\rho_m}{\rho_p} \frac{\omega_m^2}{\omega_p^2}$$

The surface tension ratio is defined by N_σ

$$N_\sigma = \frac{\sigma_p}{\sigma_m} \tag{42}$$

Thus

$$N_L^3 = \frac{N_\sigma}{N_\rho} N_T^2 \tag{43}$$

Design of a Sloshing Model

It has already been shown in the section dealing with theory that viscous effects are often neglected in the analysis of sloshing in smooth-walled tanks. Thus the Reynolds number condition would not apply. In addition, if the tank is not miniature in size or acceleration of the system is not much lower than normal gravity, then the Weber number condition does not apply.

Thus, only the first six terms in Table 2 need be considered for modelling such a system. Equations (35) to (39) apply directly. The last of these may be simplified if the value of the time scale from equation (37) is substituted. The resulting equation then is

$$N_p = N_\rho N_L N_g \tag{44}$$

The scales that apply to such a tank design are listed in Table 3.

From examination of Table 3 it is evident that a model of any reasonable size may be used with a liquid of low viscosity to simulate sloshing. The time scale for any phenomena will depend on the length and acceleration scales, while the pressure scale will depend on these and the density scale. A more important point to note is that any fluid may be used in the model, as long as it has low viscosity and surface tension.

If baffles are used in a tank, then viscous effects must be considered, even for fluids with low viscosity, and the problem becomes more complicated. It is then necessary to satisfy the condition imposed by

Reynolds number, equation (41). If the time scale is eliminated between this equation and equation (39) based on Froude number, the resulting equation defines the length scale required.

$$N_L = \frac{N_\mu^{2/3}}{N_\rho^{2/3} N_g^{1/3}} \tag{45}$$

Now it is evident that an arbitrary length scale can no longer be used. An effort is generally made to select a liquid such that its properties will result in a reasonable length scale.

Table 3. Similitude relations for model design neglecting viscosity and surface tension.

No.	Variable involved	Scale
1	Geometry	$N_L = \frac{l_p}{l_m}$
2	Time	$N_T = \frac{t_p}{t_m} = \frac{\omega_m}{\omega_p}$
3	Acceleration	$N_g = \frac{N_L}{N_T^2}$
4	Pressure	$N_p = \frac{N_\rho N_L^2}{N_T^2} = N_\rho N_L N_g$

It may be noted that if the same fluid is used in the model as in the prototype, then for tests at the same g loadings, models would have to be full size. A convenient situation arises for the case of low-g loadings for the prototype, since smaller models can then be used. In general, it is possible to simulate relatively few cases. In a situation investigated by Abramson and Ransleben (2), the prototype fluid was kerosene and the only suitable model fluid was methylene chloride CH_2Cl_2. This gave a fixed length scale of 4.21 for simulation in a one-g field.

Commonly, the Reynolds and Froude number can not both be satisfied. Since the Froude number is very basic to sloshing, the Reynolds number condition is not satisfied. It may then be reasonable to design a distorted model so that the baffles would be changed in size or configuration in order to have an effect representative of the prototype. At present so little is known about baffle design that such an approach would be unrealistic, except to draw general conclusions.

If a suitable length scale can be found, then the time and pressure scales can be found from the basic equations. Table 4 lists the scales involved for simulation including viscous effects.

Within the framework of the choice of a length scale, it may still be possible to vary the g-scale.

Consider now the case of satisfying the Weber number in addition to the Froude and Reynolds numbers. If the time scale is eliminated from equation (43) by using equation (39) then the resulting equation is

$$N_\sigma = N_L^2 N_\rho N_g \tag{46}$$

The value of the length scale may be substituted from equation (45) which

still holds.

Thus

$$N_\sigma = \left[\frac{N_\mu N_g}{N_\rho}\right]^{1/3} N_\mu \tag{47}$$

It is convenient to solve this for the g scale that is being simulated.

$$N_g = \frac{N_\sigma^3 N_\rho}{N_\mu^4} \tag{48}$$

The length scale can thus be found for this case

$$N_L = \frac{N_\mu^2}{N_\rho N_\sigma} \tag{49}$$

Table 4. Similitude relations for model design including viscous effects.

No.	Variable involved	Scale
1	Geometry	$N_L = \frac{N_\mu^{2/3}}{N_\rho^{2/3} N_g^{1/3}}$
2	Time	$N_T = \frac{N_L^{1/2}}{N_g^{1/2}}$
3	Pressure	$N_p = N_\mu^{2/3} N_g^{2/3} N_\rho^{1/3}$

This value agrees with the previous length scale, except that a particular g-scale is now also enforced. Table 5 lists the similitude requirements for full simulation of sloshing.

Table 5. Similitude including acceleration, viscous and surface tension effects

No.	Variable involved	Scale
1	Geometry	$N_L = \frac{N_\mu^2}{N_\rho N_\sigma}$
2	Acceleration	$N_g = \frac{N_\sigma^3 N_\rho}{N_\mu^4}$
3	Time	$N_T = \frac{N_\mu^{5/3}}{N_\rho N_\sigma^2}$
4	Pressure	$N_p = N_\rho N_\mu^{2/3} N_\sigma^2$

It has already been pointed out that for most cases of sloshing, the surface tension effects may be neglected. If the gravitational effect is reduced, however, then surface tension forces become comparatively more important and may have a pronounced effect on sloshing. Such a situation

may arise in the case of spacecraft when the vehicle is beginning re-entry or is maneuvering while in orbit. The effective acceleration may then vary from the normal g or higher value down to zero.

For very low values of the acceleration or when the craft is weightless, the surface tension effects predominate and any liquid will tend to either form a sphere or to wet the inside surface of the tank. Tests carried out by Petrash et al. (30) show that an equilibrium condition is achieved for the case of mercury as a non-wetting fluid or water as a wetting fluid in fractions of a second for containers of 2 or 3 inches in diameter. A certain amount of oscillation about the equilibrium position may be present, but such motion is due to the interaction of surface tension and inertia forces and is not considered here.

Consider a spacecraft in orbit, performing a rendezvous or re-entry maneuver. As the g-forces build up, the liquid inside any tank will be subjected to an increasing acceleration until a point is reached when the surface tension effect is overcome and the fluid flows around to a new configuration. Because of the dynamic action a certain amount of oscillation or sloshing would be expected. At the same time, if the vehicle is in a planetary atmosphere, buffeting and stability problems present themselves. Sloshing under such conditions has not been investigated and so is of some interest to consider because the condition could well be a critical one.

Information on the effect of surface tension on fluid behavior under weightlessness has been obtained recently. Petrash et al. (29) report on the result of tests carried out in the MA-7 spacecraft flight. In this

experiment a model tank was carried in a Mercury Capsule and observed during re-entry. It was found that at a g-loading of 0.30 the fluid transferred its mode of behavior rather abruptly from surface tension to gravitational control. However, in this report the authors did not relate this critical value to the fluid properties and container size. A more significant critical number can be obtained by application of similitude to the problem. The significant variables involved are the liquid properties σ and ρ, the effective acceleration γ and the vessel diameter a. A suitable dimensionless parameter that relates gravitational to surface tension forces is $\frac{\rho\gamma a^2}{\sigma}$. This parameter may also be developed from the Weber and Froude numbers. Thus

$$C = \frac{W}{F} = \frac{\rho\gamma a^2}{\sigma} \tag{50}$$

where C is the dimensionless number that defines the relative gravity action to the surface tension effect.

The critical value of this number may be obtained from the data on the MA-7 experiment as reported by Petrash *et al.* (29).

ρ = 1 gm/cm^3 (distilled water)

g = 980 cm/sec^2 (standard value)

γ = 0.30 g = 294 cm/sec^2 (observed)

a = 1.1 inches = 2.8 cm

σ = 73 dynes/cm

Thus

$$C_c = \frac{\rho\gamma a^2}{\sigma} = 31.4 \tag{51}$$

This is the value of C for the critical or transition point between

surface tension and gravity control. If C is greater than 31.4 then acceleration influenced sloshing may occur.

It is not expected that this value is particularly accurate since it is based on only one experiment, which was not designed for this purpose. However, this result should indicate the sort of value that is expected, and more experiments would establish an accurate figure.

Sloshing under the conditions described above would have to be investigated for various cases, including landings on other bodies in our planetary system since water, fuel and other liquids would have to be transported. In order to design a proper model for simulation of sloshing under such conditions, a study was made of liquids which may be used.

Sloshing with Surface Tension Effects

Just after transition from a surface tension to a gravity controlled motion of the fluid, the effect of surface tension is still present to a noticeable degree. Thus model study should include this effect in the proper proportion. Table 5 lists the equations that govern such a model design.

Table 6 contains a list of propellants, other useful liquids and suggested model fluids. The data was obtained from Abramson and Ransleben (2) and Sandorff (34).

Tables 7 to 10 list the length scale and acceleration scale that would result if four different fluids are used for the model analysis.

These tables have to be used in conjunction with the critical value of the parameter C. The fluid has to be gravity controlled but not

overwhelming so. Thus the size of the prototype or the model has to be known in order that C may be found (Equation 50). Simulation of gravity controlled sloshing will then be valid only for the case where C is only slightly greater than C_c.

It is of interest, however, to consider the possible useful cases. Table 7 indicates that it may be possible to use water in a model to simulate sloshing of ethyl alcohol under low-g conditions. From Table 8, it may be concluded that methylene chloride could be used to simulate hydrogen peroxide and water. Table 9 shows that liquid ammonia might be used to simulate water and possibly hydrogen peroxide. Mercury might be used to simulate liquid ammonia according to Table 10. Note that the length scale or the acceleration scale may make simulation impractical.

Table 6. Properties of some fluids used in spacecraft or for models.

No.	Liquid	Temperature Degree F	Density gm/cm^3	Viscosity poises	Surface Tension dynes/cm
1	Liquid hydrogen	-439	0.071	0.00013	1.9
2	Hydrogen peroxide	68	1.44	0.0125	76
3	Ethyl alcohol	68	0.79	0.012	22
4	Liquid ammonia	- 28	0.68	0.0026	34
5	Liquid oxygen	-297	1.14	0.0019	13
6	Water	68	0.998	0.010	73
7	Methylene chloride	68	1.34	0.0044	27
8	Mercury	68	13.56	0.016	476

Table 7. Similitude based on water for the model.

No.	Liquid	N_L	N_g
1	Liquid hydrogen	0.0092	9.57
2	Hydrogen peroxide	1.01	1.45
3	Ethyl alcohol	6.04	0.18
4	Liquid ammonia	0.21	0.26
5	Liquid oxygen	0.18	0.634
6	Water	1.0	1.0
7	Methylene chloride	0.39	0.15
8	Mercury	0.029	2460

Table 8. Similitude based on methylene chloride for the model.

No.	Liquid	N_L	N_g
1	Liquid hydrogen	23.4	0.0024
2	Hydrogen peroxide	2.65	0.368
3	Ethyl alcohol	15.6	0.056
4	Liquid ammonia	0.54	8.47
5	Liquid oxygen	0.45	2.75
6	Water	2.56	0.56
7	Methylene chloride	1.0	1.0
8	Mercury	0.06	390

Table 9. Similitude based on liquid ammonia for the model.

No.	Liquid	N_L	N_g
1	Liquid hydrogen	44.6	0.003
2	Hydrogen peroxide	4.92	0.04
3	Ethyl alcohol	28.3	0.0007
4	Liquid ammonia	1.0	1.0
5	Liquid oxygen	0.83	0.33
6	Water	4.72	0.06
7	Methylene chloride	1.84	0.12
8	Mercury	0.14	37.6

Table 10. Similitude based on mercury for the model.

No.	Liquid	N_L	N_g
1	Liquid hydrogen	3×10^{-12}	$8.12(10)^{-14}$
2	Hydrogen peroxide	34.7	0.0012
3	Ethyl alcohol	209	0.0018
4	Liquid ammonia	7.43	0.026
5	Liquid oxygen	6.21	0.0085
6	Water	34.5	0.0007
7	Methylene chloride	25.2	0.0009
8	Mercury	1.0	1.0

EXPERIMENTAL PROCEDURE

Description of Apparatus

The vessel used for the experiments was a rectangular tank, ten inches long, six inches wide and fifteen inches high. It was made of clear plastic so that the liquid surface could be observed and photographed. A pitching motion about the center of gravity of the liquid was required, but a fixed pivot point was not considered suitable. A solution was obtained by using two circular segments attached at the bottom of the container as shown in Figs. (4) to (7).

These segments ride on roller bearings and thus permit a rotation of the tank about the center of their profile. The rotational center can be maintained at the liquid center of gravity by building up the bottom of the container to an appropriate height depending on the liquid level required.

The container was oscillated by a simple link attached to a vertical shaker table. The shaker unit was part of a commercial system developed for vibration testing and had a completely mechanical system for obtaining the vertical motion. An independent check of the operation of the table established that a smooth sinusoidal motion is generated.

The amplitude of vertical motion could be set at any value from zero to 0.10 inches. Since the moment arm for rocking the table was 12 inches, the corresponding maximum angular deflection β of the tank was 0.00833 radians. Thus even at this maximum value of excitation, the forcing motion could still be considered small.

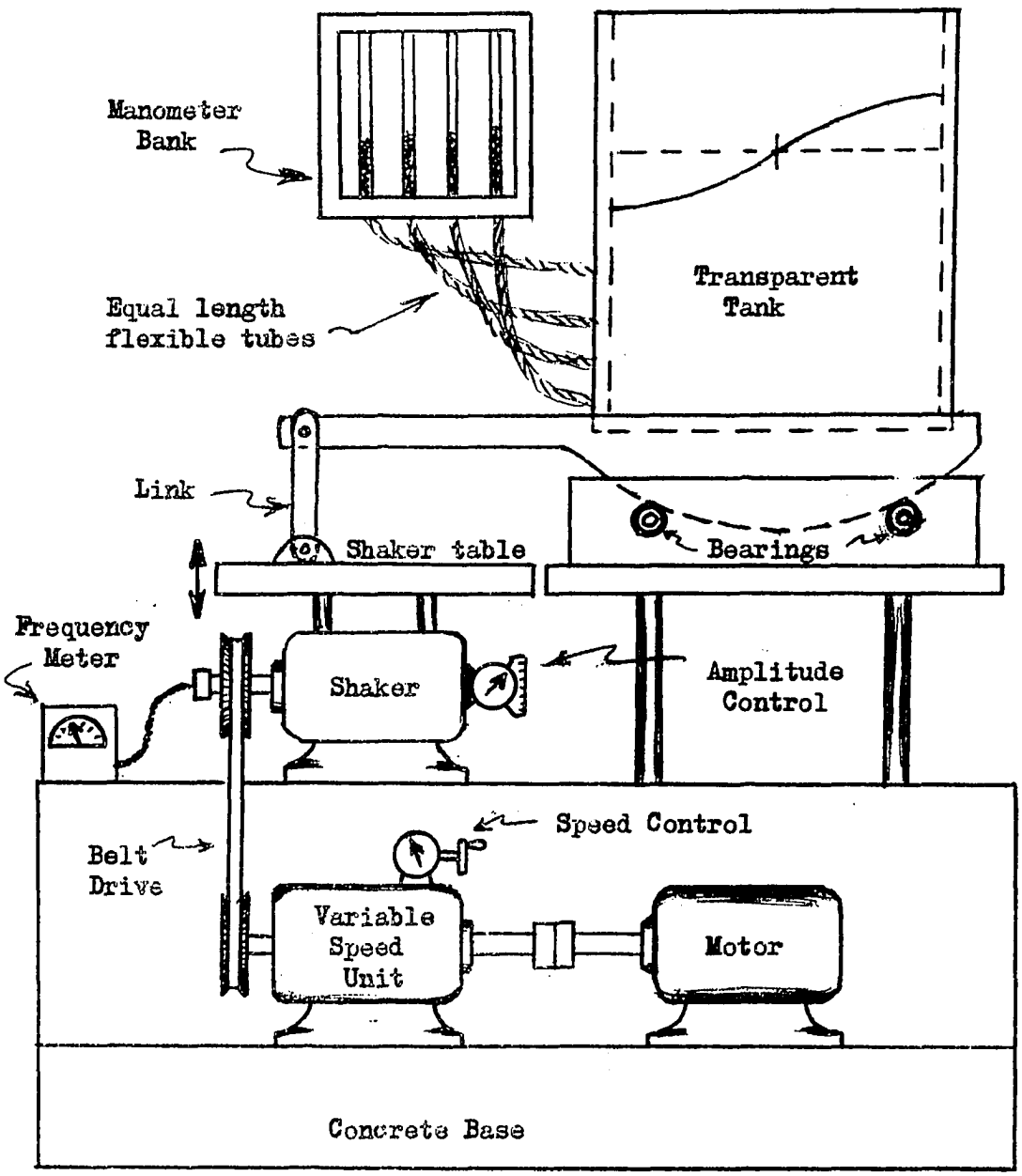

Fig. 4. Schematic diagram of sloshing apparatus

Power was supplied to the table by a 3/4 hp electric motor driving a variable speed unit which in turn was connected to the shaker by a V-belt. The frequency of oscillation could be varied from zero to 300 cycles per minute. Since the drive system was much larger than required for a shaker of this size, very stable frequency control could be maintained.

The complete unit was mounted on a concrete block weighing nearly two tons. No problems of unwanted vibrations were present and after careful adjustment, the vessel motion was very regular and smooth.

Conduct of Experiments

Two types of boundary exist for the fluid in the vessel. A free surface at constant pressure, and a solid surface at the tank wall. To check the solution, it was desirable to take measurements around the complete boundary.

The wave profile for the free surface was established by visual means. A wax crayon was used to mark the position of the liquid surface at maximum displacement. The wave form could also be obtained by dipping cards into the liquid and observing the wetted portion. For a simple mode, the card could be left in for several cycles and would show the upper portion of the wave on each half of the centerline. At low frequencies, a card was dipped in quickly to obtain a trace of the full wave form.

Photographing the surface at an extreme position proved rather difficult, so that random pictures were taken in much the same manner as reported by Taylor (43). Since the amplitude scale was easy to check

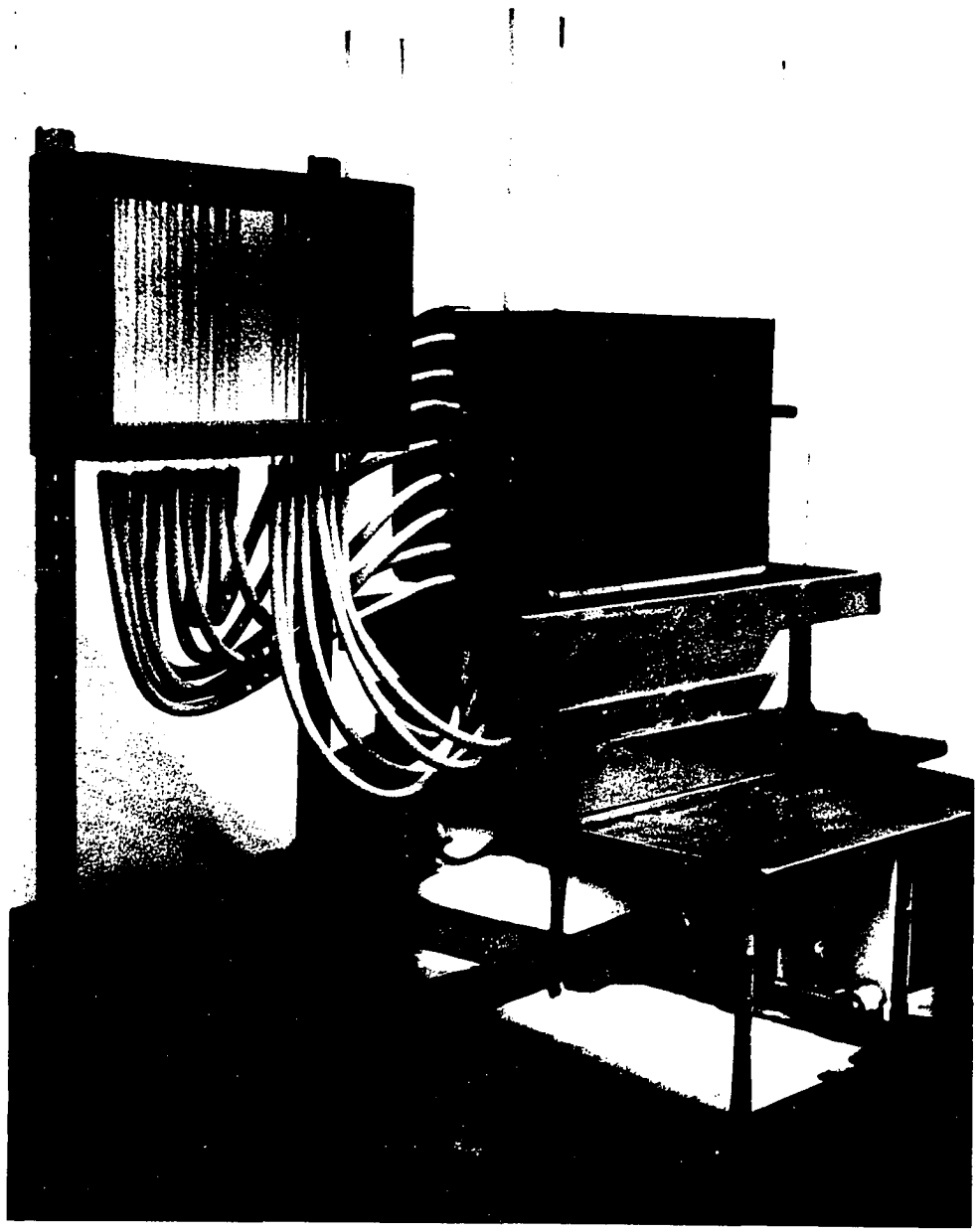

Fig. 5. Sloshing apparatus
General view

independently, such photographs were considered quite suitable for obtaining the wave form of the oscillating liquid, even though the displacement may be less than the maximum value. A dye was used in the water so that the liquid surface would stand out clearly.

An interesting sidelight during this portion of the experimental work was the proof that the liquid surface passed through the undisturbed flat condition during the sloshing motion. Two of the many random photographs that were taken show a flat, apparently motionless surface. In one case the motion was in the first mode and in the large amplitude or non-linear range. In the second case the motion was in the second mode but again only a flat surface appears on the photograph.

Movies of the sloshing motion were also taken but it was not found convenient nor necessary to take measurements from them.

The dynamic pressure along the sides and bottom was measured by using manometer tubes connected to openings along the tank surface. All the tubes were made the same length so that the response would be the same for each one. This arrangement was used by Hoskins and Jacobsen (15) in their study of fluid motion in a container which was oscillated horizontally to simulate a dam during an earthquake. Hoskins and Jacobsen used manometers with a total length of about three feet and were able to obtain good results. Better response can be obtained with a shorter length and a length of 14 inches was used in the apparatus described here. The method can be used with reasonable success for pressure measurements at low frequency. At higher frequencies, the manometer response drops off and precludes accurate measurement even

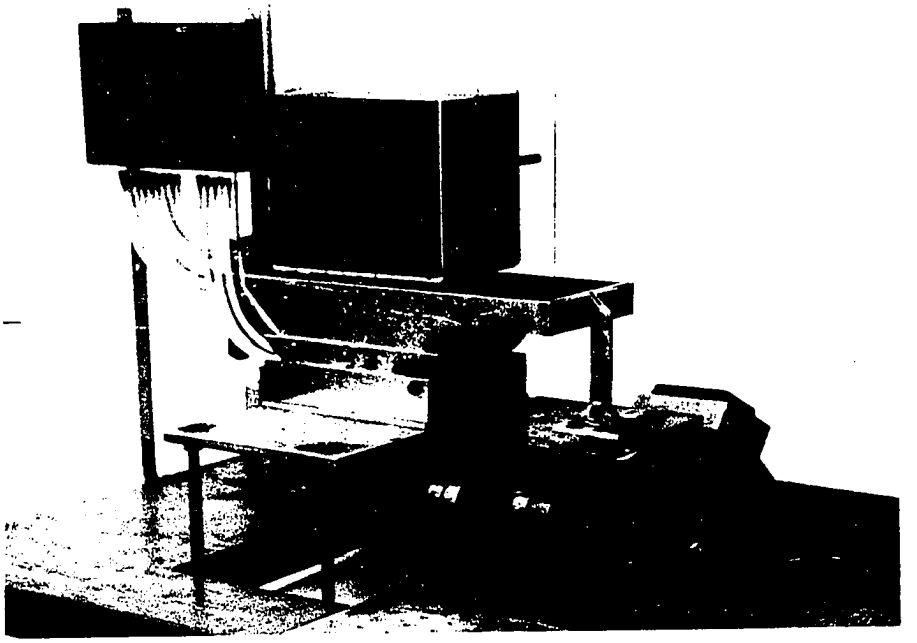

Fig. 6. Sloshing apparatus

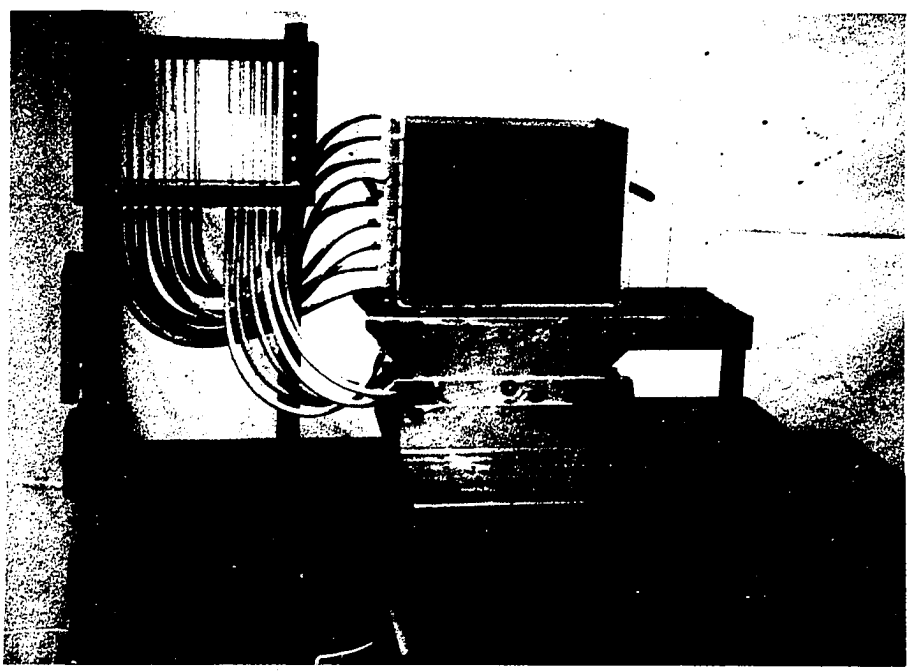

Fig. 7. Sloshing apparatus

though a correction can be applied. No other method of measuring the small and oscillating pressures was available so that readings had to be confined to the first sloshing mode. This restriction was not considered too serious, however, since the first mode of oscillation is the most important one in most design applications. Furthermore a reasonable check of the theory was carried out at higher frequencies by measurement of the free surface shape.

RESULTS AND DISCUSSION

Analytical Results

The natural frequency of fluid sloshing in a pitching vessel is given by equation (30). For presenting results it is preferable to use the dimensionless form of this equation.

$$\frac{\omega_n^2 a}{\gamma} = \pi(2n-1) \tanh\left[\pi(2n-1)\frac{h}{a}\right] \quad \text{for } n = 1, 2, 3, \ldots \qquad (52)$$

The solution for the first four sloshing modes is given in Table 11. The dimensionless frequency $\frac{\omega_n^2 a}{\gamma}$ is presented as a function of various h/a ratios. The results are also shown in graphical form in Fig. 14.

Table 11. Calculated frequency $\frac{\omega_n^2 a}{\gamma}$ as a function of h/a

h/a	n = 1	n = 2	n = 3	n = 4
0.1	0.955	6.94	14.4	21.45
0.2	1.75	9.00	15.6	22.0
0.4	2.67	9.40	15.7	22.0
0.6	2.99	9.42	15.7	22.0
0.8	3.10	9.42	15.7	22.0
1.0	3.14	9.42	15.7	22.0
1.2	3.15	9.42	15.7	22.0

Tables 12 to 15 present the calculated values of the wave height as a function of x/a for four h/a ratios. Again the wave height is presented as a dimensionless ratio $\frac{\eta_o}{a\beta}$. This term is obtained from equation (32)

with the values of F_1 and F_2 substituted in. Values were calculated for a frequency range that includes the two lowest sloshing modes.

The curves in Figures 8 to 11 show a graphical representation of this data. Only one half of the wave motion is shown since in all cases the wave is skew-symmetrical. The phase of the motion is evident from the sign of the amplitude. Since viscous effects have been neglected, the phase is either zero, represented by a negative amplitude, or 180 degrees, in which case the amplitude is positive. Thus, up to the first resonance peak the motion of the wave is in phase with the applied disturbance. As this resonance frequency is passed, the phase undergoes a change to 180 degrees. A similar change occurs at each natural frequency although only a part of the wave changes phase. This result is completely analogous to the forced vibration of a distributed mass system such as a stretched string.

The data in Tables 16 and 17 represent the pressure distribution along the end walls and bottom of the pitching vessel. These results were calculated only for the ratio $h/a = 0.8$. This was done since experimental pressure measurements were best verified for the case of a container that was fairly well filled.

The pressure is presented as a dimensionless value $\frac{p_d}{\rho a^2 \omega^2 \beta}$. This expression is obtained from equation (33) with appropriate values of F_1 and F_2 substituted in. The curves in Fig. 12 and 13 show a graphical version of this data. It is of some interest to compare these curves with the curves in Fig. 11 showing the wave shape for the same case.

Table 12. Calculated $\frac{\eta_o}{a\beta}$ as a function of ω and x for h/a = 0.1

ω \ x/a	0.1	0.2	0.3	0.4	0.5
2	-0.015	-0.028	-0.037	-0.045	-0.048
4	-0.091	-0.173	-0.238	-0.284	-0.300
6	-4.75	-9.095	-12.50	-14.75	-15.5
8	0.290	0.547	0.742	0.864	0.904
10	0.205	0.379	0.505	0.576	0.598
11	0.190	0.349	0.454	0.510	0.526
12	0.188	0.341	0.434	0.476	0.485
16	0.715	0.943	0.589	0.016	-0.159
18	-0.006	0.093	0.301	0.518	0.611
19	0.037	0.144	0.316	0.480	0.549
20	0.055	0.164	0.320	0.460	0.518
22	0.071	0.181	0.320	0.438	0.483

Table 13. Calculated $\frac{\eta_o}{a\beta}$ as a function of ω and x for h/a = 0.2

ω \ x/a	0.1	0.2	0.3	0.4	0.5
2	-0.007	-0.013	-0.017	-0.020	-0.021
4	-0.031	-0.060	-0.084	-0.099	-0.105
6	-0.118	-0.225	-0.311	-0.367	-0.387
8	-1.803	-3.44	-4.73	-5.56	-5.85
10	0.328	0.622	0.851	0.994	1.045
11	0.244	0.460	0.624	0.727	0.763
12	0.207	0.387	0.521	0.603	0.632
16	0.172	0.307	0.385	0.415	0.420
18	0.298	0.459	0.406	0.294	0.235
19	-0.154	-0.085	0.230	0.597	0.760
20	0.041	0.143	0.297	0.445	0.505
22	0.077	0.185	0.307	0.399	0.432

Table 14. Calculated $\frac{\eta_o}{a\beta}$ as a function of ω and x for h/a = 0.4

ω \ x/a	0.1	0.2	0.3	0.4	0.5
2	-0.003	-0.005	-0.007	-0.008	-0.009
4	-0.012	-0.023	-0.032	-0.037	-0.039
6	-0.035	-0.067	-0.093	-0.109	-0.115
8	-0.108	-0.206	-0.284	-0.333	-0.351
10	-2.35	-4.47	-6.15	-7.23	-7.60
11	0.436	0.829	1.141	1.338	1.409
12	0.230	0.437	0.600	0.704	0.740
16	0.114	0.214	0.290	0.336	0.351
18	0.110	0.200	0.257	0.286	0.293
19	0.401	0.538	0.358	0.061	-0.085
20	0.080	0.156	0.224	0.258	0.262
22	0.076	0.150	0.215	0.249	0.261

Table 15. Calculated $\frac{\eta_o}{a\beta}$ as a function of ω and x for h/a = 0.8

ω \ x/a	0.1	0.2	0.3	0.4	0.5
2	-0.001	-0.001	-0.002	-0.002	-0.002
4	-0.003	-0.006	-0.008	-0.010	-0.010
6	-0.009	-0.017	-0.023	-0.027	-0.028
8	-0.023	-0.044	-0.061	-0.072	-0.076
10	-0.105	-0.199	-0.274	-0.322	-0.339
11	1.515	2.88	3.96	4.66	4.90
12	0.118	0.225	0.310	0.364	0.383
16	0.038	0.072	0.099	0.116	0.123
18	0.032	0.061	0.084	0.098	0.104
19	0.031	0.057	0.079	0.093	0.098
20	0.029	0.055	0.075	0.088	0.093
22	0.027	0.050	0.070	0.082	0.086

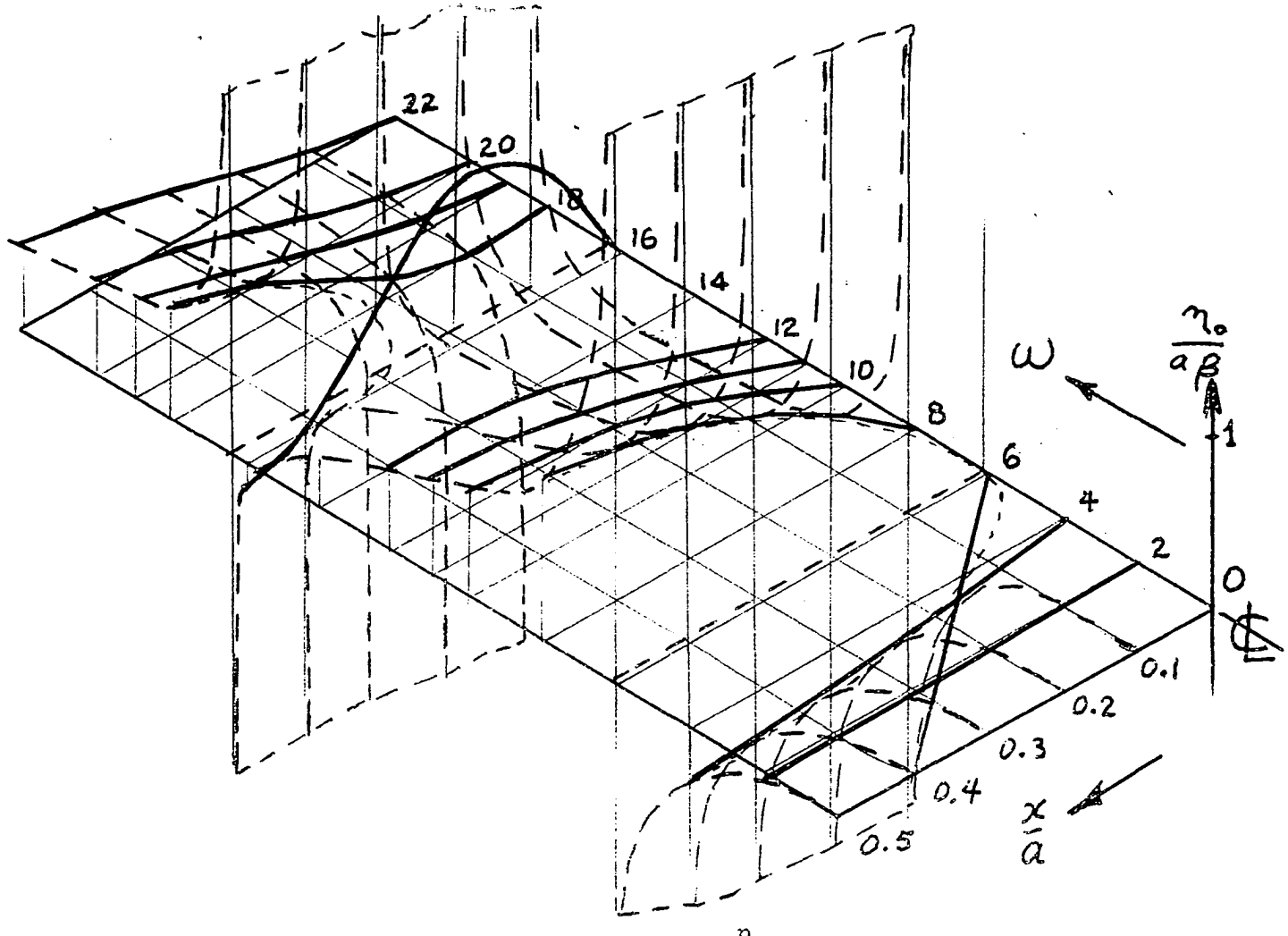

Fig. 8. Calculated wave height $\frac{\eta_o}{a\beta}$ as a function of ω and x for h/a = 0.1

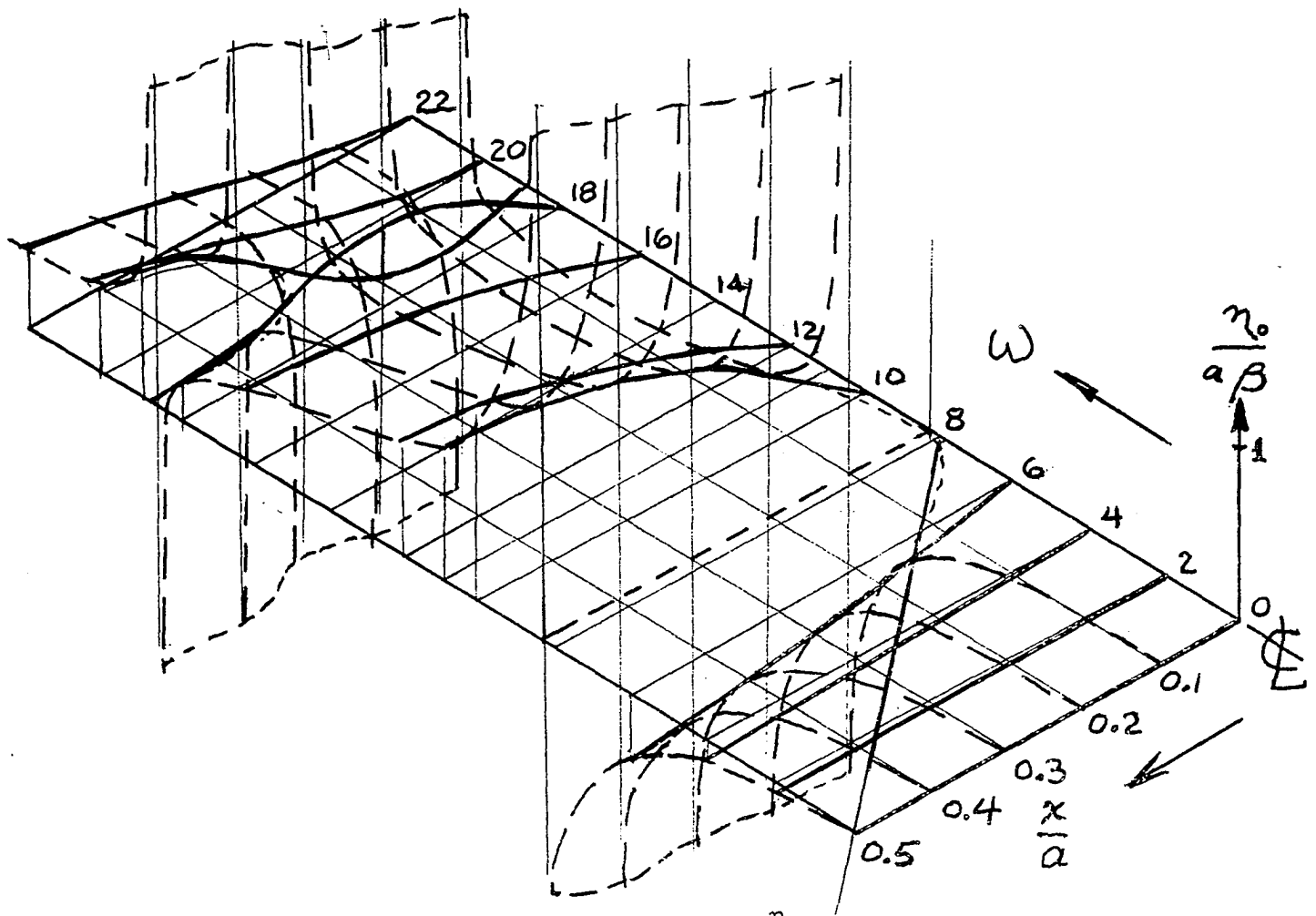

Fig. 9. Calculated wave height $\frac{\eta_o}{a\beta}$ as a function of ω and x for h/a = 0.2

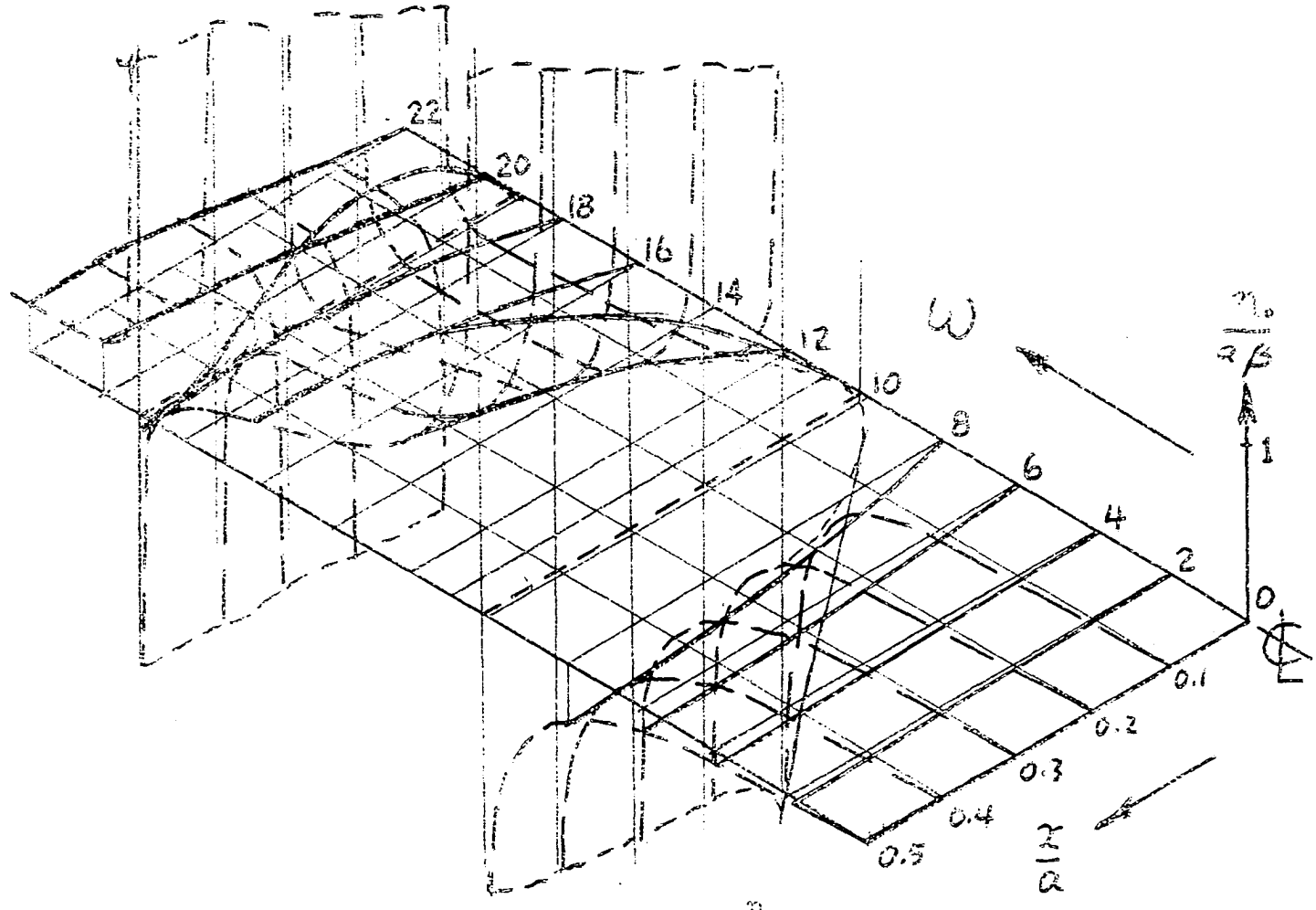

Fig. 10. Calculated wave height $\frac{\eta_o}{a\beta}$ as a function of ω and x for h/a = 0.4

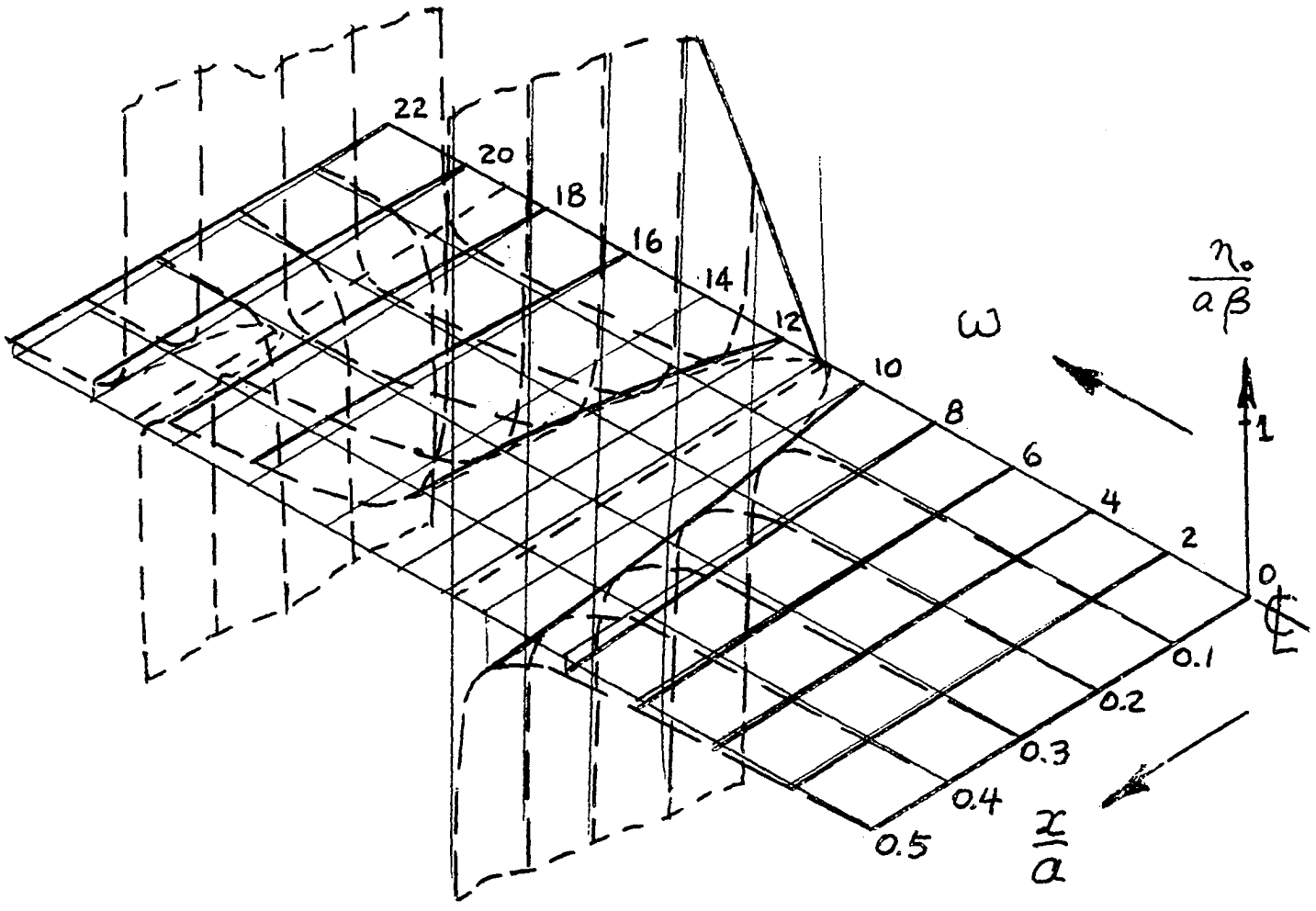

Fig. 11. Calculated wave height $\frac{\eta_0}{a\beta}$ as a function of ω and x for h/a = 0.8

Table 16. Calculated dynamic pressure $\frac{p_d}{\rho a^2 \omega^2 \beta}$ along bottom of vessel as a function of ω and x/a for $h/a = 0.8$

ω \ x/a	0	0.1	0.2	0.3	0.4	0.5
4	0	0.029	0.053	0.070	0.075	0.044
8	0	0.029	0.046	0.060	0.060	0.026
10	0	0.029	0.054	0.071	0.074	0.040
11	0	-0.121	-0.233	-0.323	-0.385	-0.445
12	0	-0.017	-0.030	-0.038	-0.034	-0.009
14	0	-0.021	-0.040	-0.052	-0.050	-0.019
16	0	-0.021	-0.041	-0.055	-0.056	-0.027

Table 17. Calculated dynamic pressure $\frac{p_d}{\rho a^2 \omega^2 \beta}$ along end wall of vessel as a function of ω and z/a for $h/a = 0.8$

ω \ z/a	0.4	0.2	0	-0.2	-0.3	-0.4
4	0.107	0.079	0.040	0.017	0.017	0.044
8	0.130	0.075	0.043	0.013	0.017	0.026
10	0.193	0.110	0.050	0.016	0.017	0.040
11	-2.044	-1.632	-0.932	-0.589	-0.536	-0.445
12	-0.056	-0.032	-0.034	-0.036	-0.031	-0.009
14	-0.006	-0.002	-0.005	-0.011	-0.006	-0.019
16	-0.008	-0.004	-0.002	-0.001	-0.001	-0.027

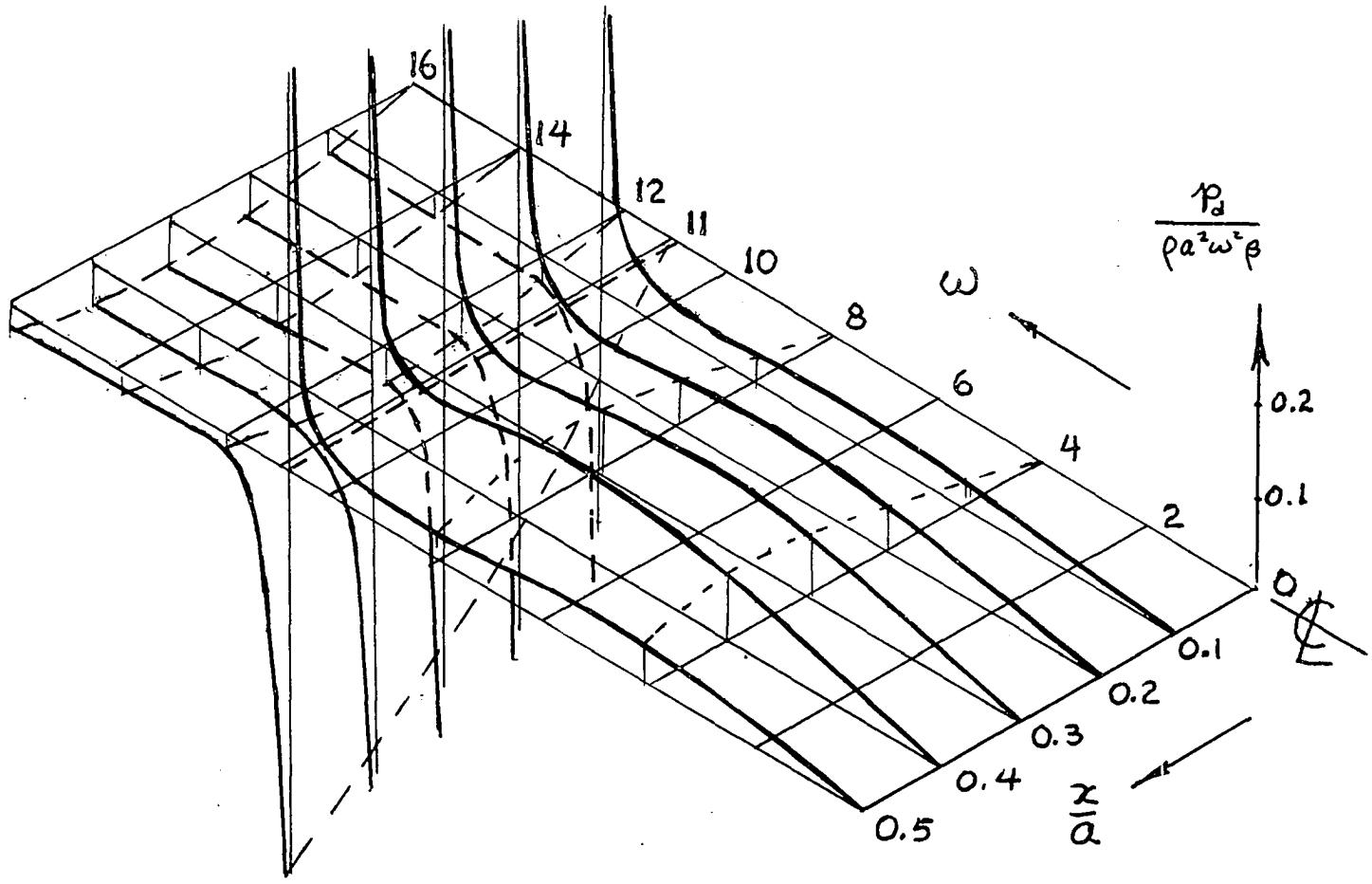

Fig. 12. Calculated dynamic pressure $\frac{p_d}{\rho a^2 \omega^2 \beta}$ along bottom of vessel as a function of ω and x/a for $h/a = 0.8$

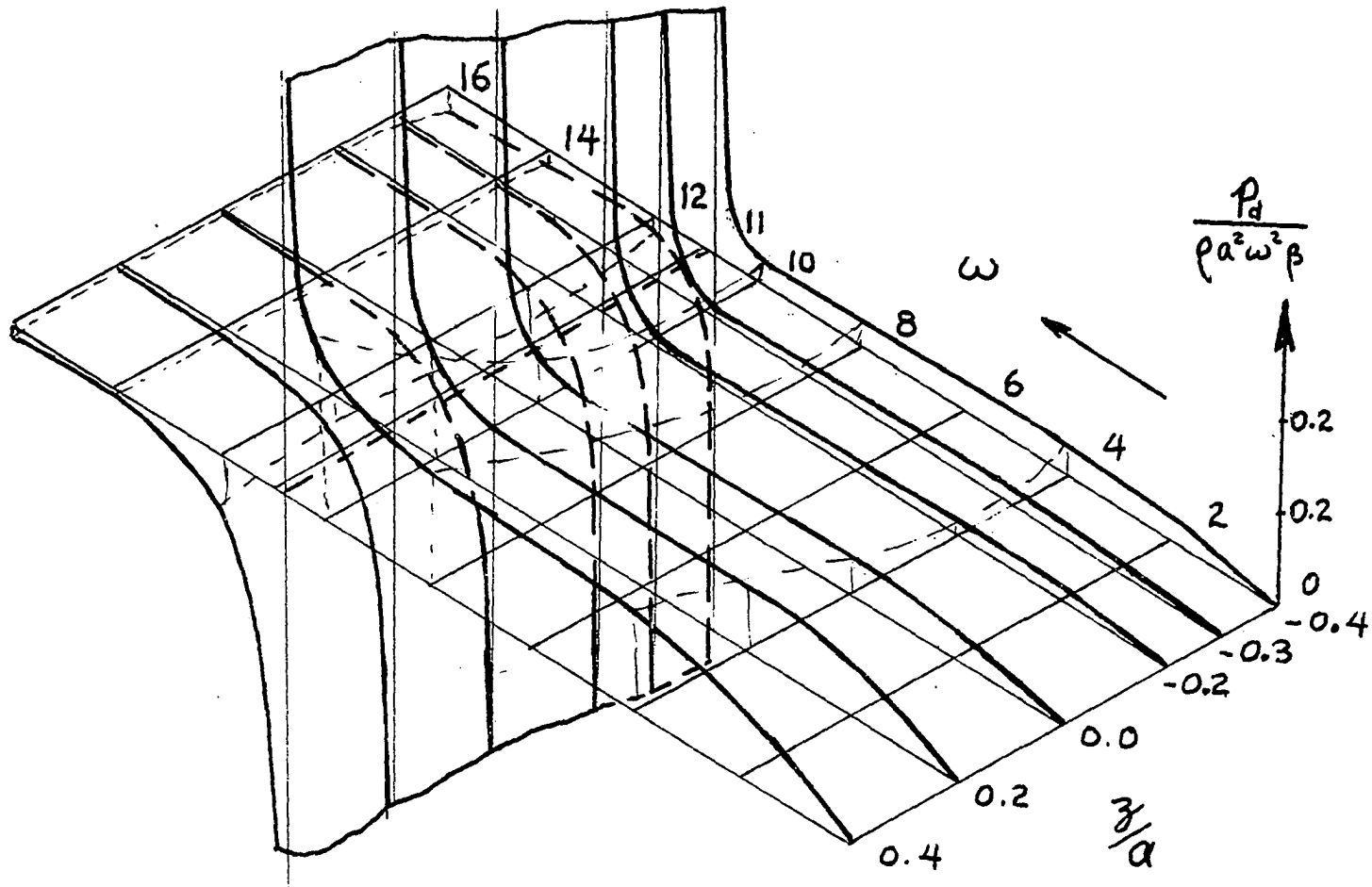

Fig. 13. Calculated dynamic pressure $\frac{p_d}{\rho a \omega^2 \zeta_\beta}$ along end wall of vessel as a function of ω and z/a for $h/a = 0.8$

Experimental Verification

The first portion of the experimental program was to check the frequency at which resonance occurs. For low h/a ratios such as 0.1, the response curve was so wide near the resonant frequency that it was difficult to obtain a value that could be considered a natural frequency. For higher h/a values, excellent agreement with theory was obtained. Fig. 14 shows the experimental values on the theoretical curves. In most cases the value of a resonant frequency was established by increasing and then decreasing frequency and observing the wave height. The average of the two figures so obtained was then used. It may be noted that the frequencies obtained experimentally tend to be somewhat lower than theoretical values.

The wave form was obtained by direct measurement on the container and from the photographs.

Figs. 15 and 16 showing the surface at zero displacement are of interest although they do not involve any measurements. The meniscus may be seen on the downward moving portion of the fluid in these photographs. The other photographs were taken near the peak of motion when velocities are low so that the meniscus appears on both downward and upward portions of the wave.

The photographs in Figs. 17 to 26 show the surface wave form for various conditions. It may be readily noted that the large amplitude motion that occurs in the vicinity of a resonance peak is in the non-linear range and departs from the theoretical form. Splashing generally occurs during such large amplitude motions.

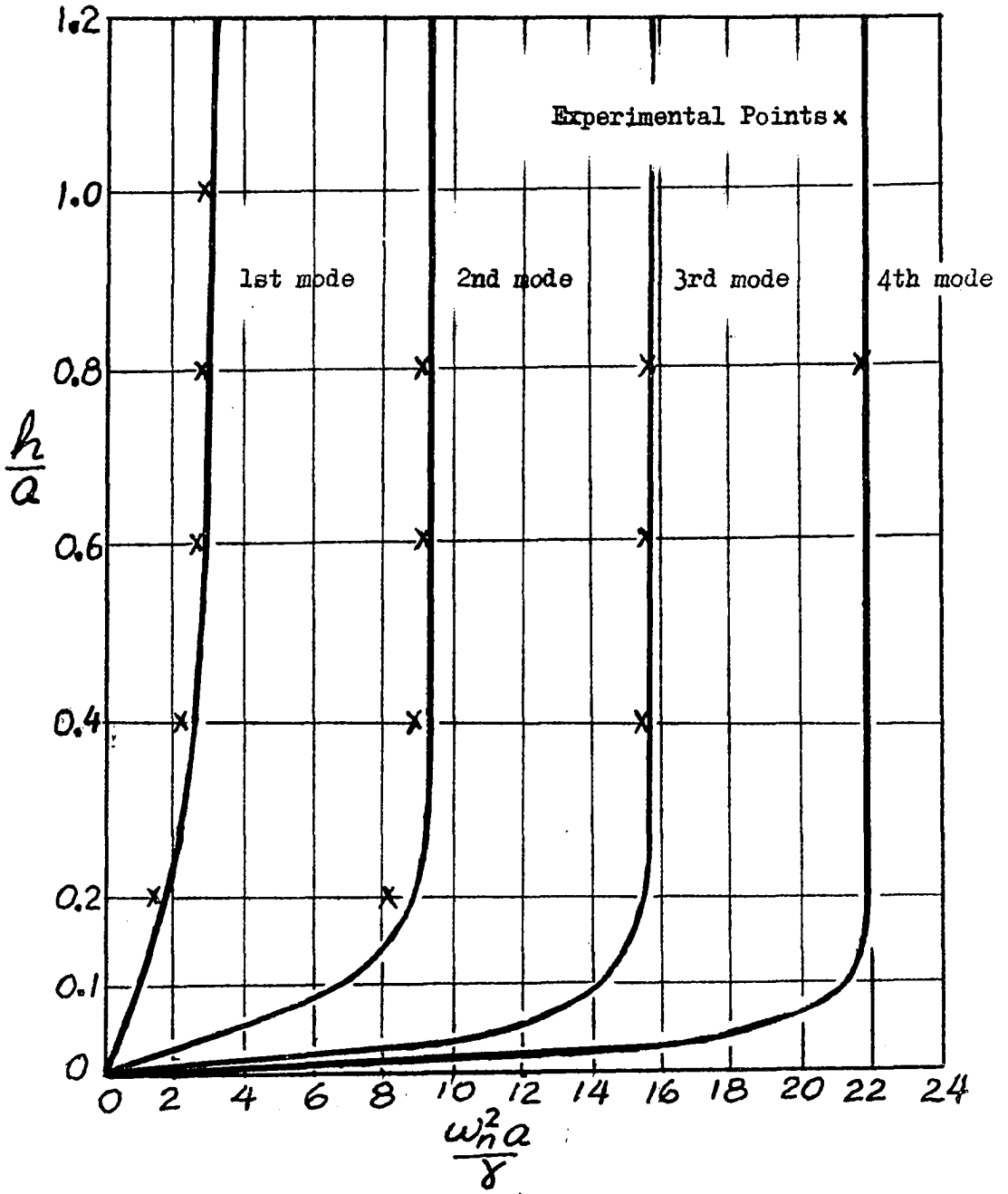

Fig. 14. Natural frequency $\frac{\omega_n^2 a}{\gamma}$ as a function of h/a

When the frequency is high, a splashing motion also occurs as shown in Figs. 27 and 28.

A comparison of theoretical and experimental wave forms is shown in Figs. 29 and 30. In all cases the experimental results show a lower amplitude than predicted by theory. This result is expected since the slight amount of damping that is present would tend to reduce the amplitude. In general, the results are considered good and show that the theory accurately predicts the wave from in a pitching vessel.

The curves in Figs. 31 and 32 present the experimental and theoretical dynamic pressure results for the end walls and bottom of the container. These results are not quite as good as the previous ones but are in reasonable agreement with theory. The fact that experimental points are lower than theoretical is attributed to two factors. The viscous damping action and the response of the manometers both would tend to give lower than theoretical values. Experimental pressure readings were all read as positive values but are plotted in the same sense as the theoretical curves to show the appropriate phase relationship.

Finally, it is of interest to note that some difficulty was experienced during the testing program due to cross motions. Thus, waves in a transverse direction would sometimes appear. In many cases such waves could be eliminated by using a divider plate to change the width of the tank. For high-amplitude motions, such remedial measures were less successful. Thus amplitude was kept low for this reason as well as for the need to satisfy the linearized equations.

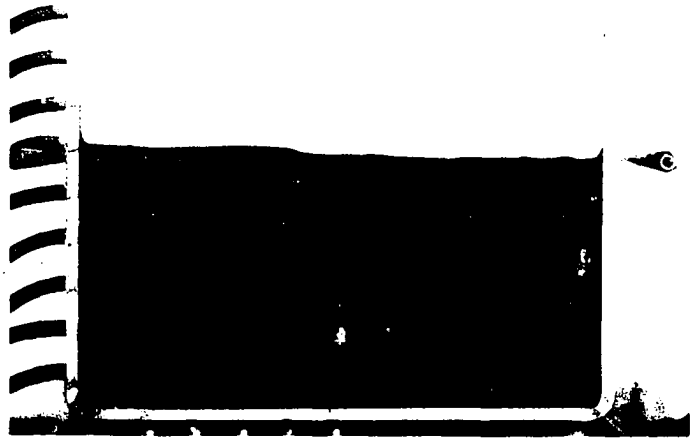

Fig. 15. Motion caught at zero displacement
First mode, h/a = 0.5

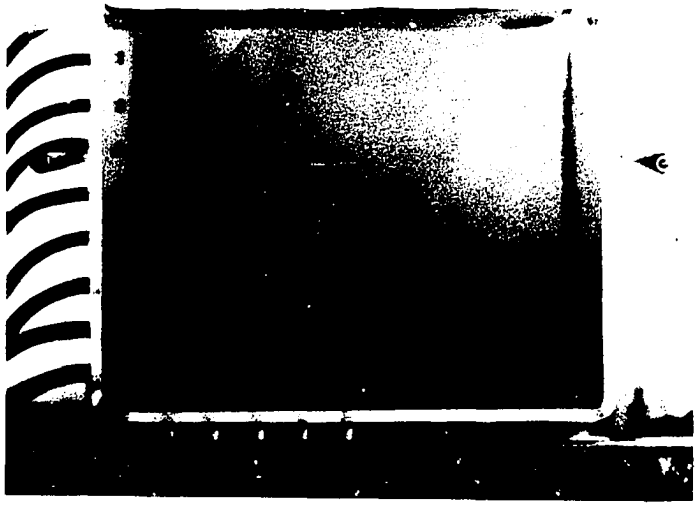

Fig. 16. Motion caught at zero displacement
Second mode, h/a = 0.8

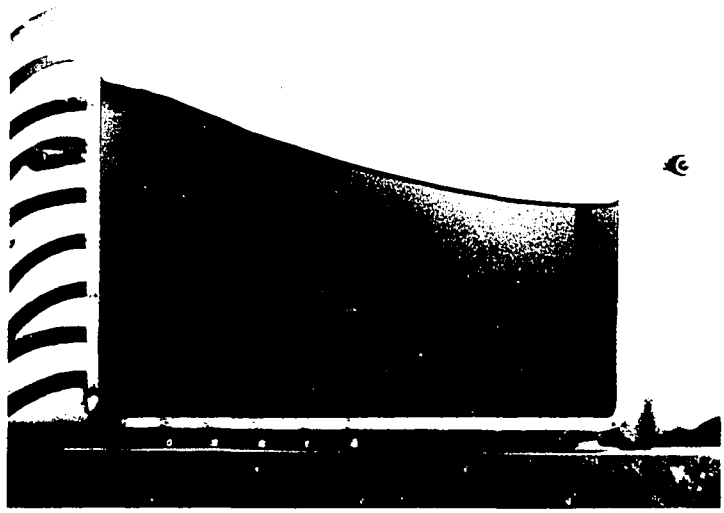

Fig. 17. Motion in first mode
Frequency = 11.5 rad/sec, $\frac{\omega^2 a}{\gamma} = 3.4$, $h/a = 0.4$

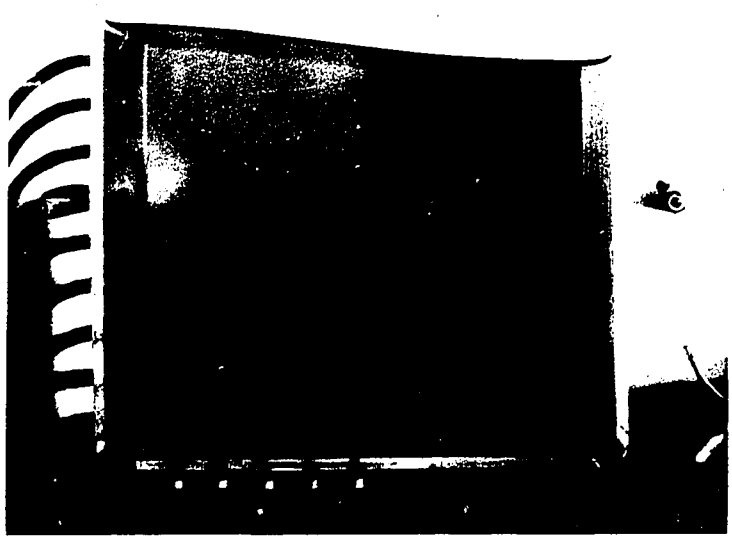

Fig. 18. Motion in first mode
Frequency = 11.5 rad/sec, $\frac{\omega^2 a}{\gamma} = 3.4$, $h/a = 0.8$

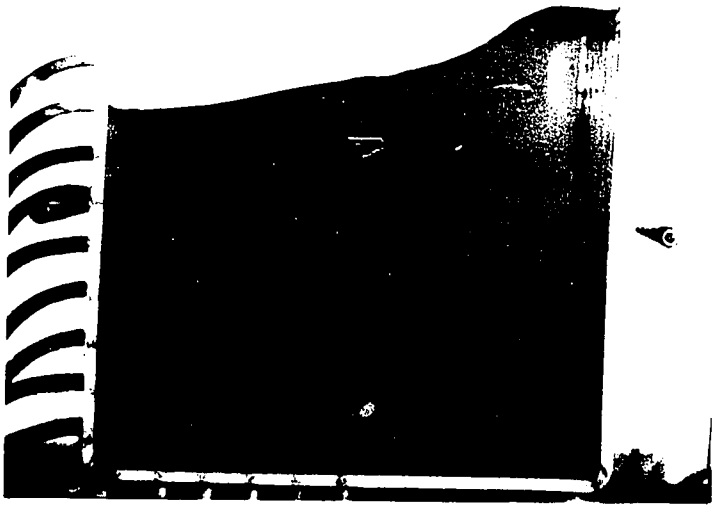

Fig. 19. Large amplitude sloshing in the first mode
Frequency approximately 10.7 rad/sec, $\frac{\omega^2 a}{g} = 3.0$, $h/a = 0.8$

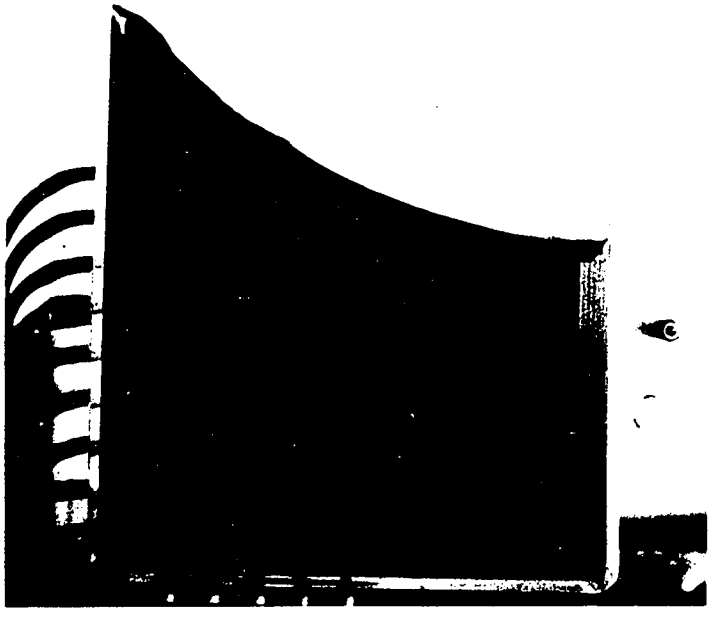

Fig. 20. Large amplitude, non-linear motion in the first mode
Frequency approximately 10.7 rad/sec, $\frac{\omega^2 a}{g} = 3.0$, $h/a = 0.8$

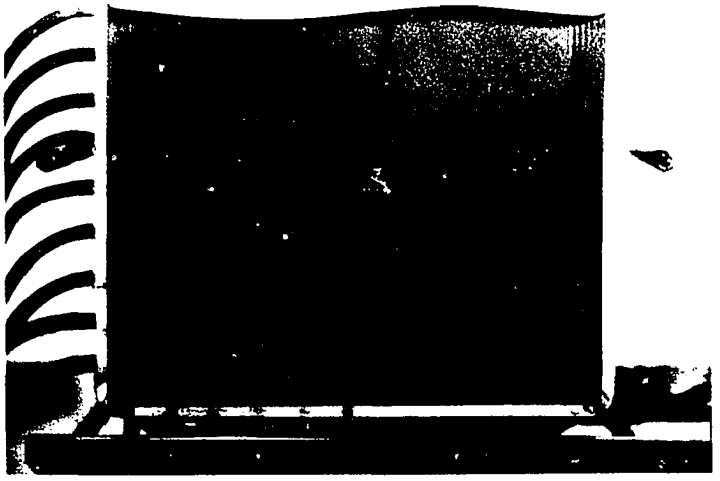

Fig. 21. Motion in the second mode
Frequency 18.7 rad/sec, $\frac{\omega^2 a}{g} = 9.1$, $h/a = 0.8$

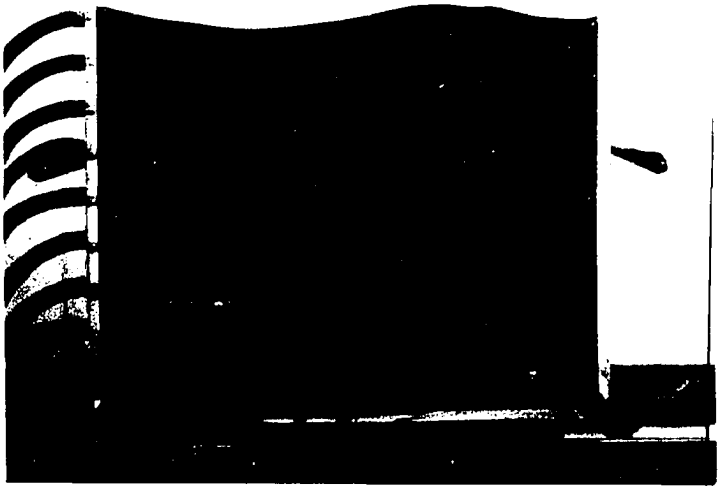

Fig. 22. Motion in the second mode
Frequency 18.7 rad/sec, $\frac{\omega^2 a}{g} = 9.1$, $h/a = 0.8$

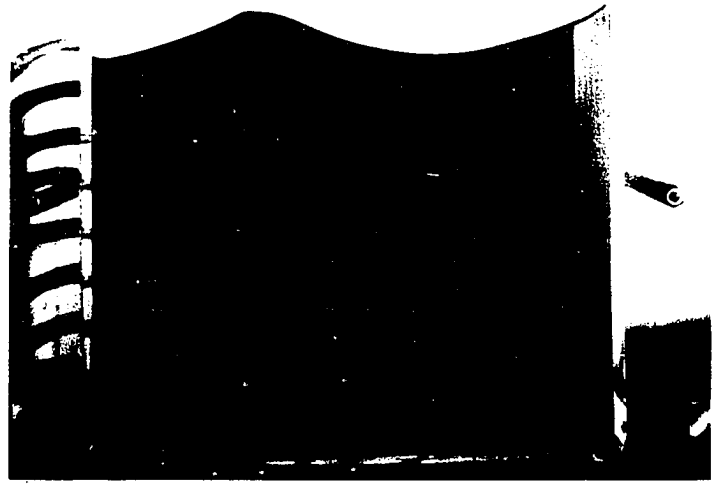

Fig. 23. Large amplitude sloshing in the second mode
Frequency 18.7 rad/sec, $\frac{\omega^2 a}{g} = 9.1$, $h/a = 0.8$

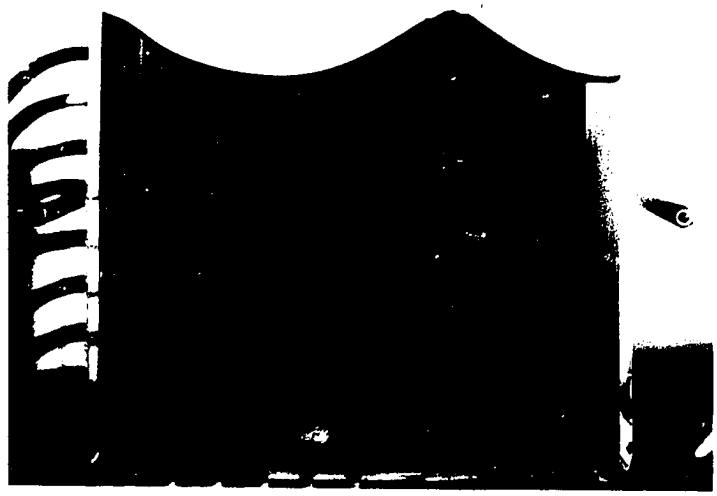

Fig. 24. Large amplitude, non-linear motion in the second mode
Frequency 18.7 rad/sec, $\frac{\omega^2 a}{g} = 9.1$, $h/a = 0.8$

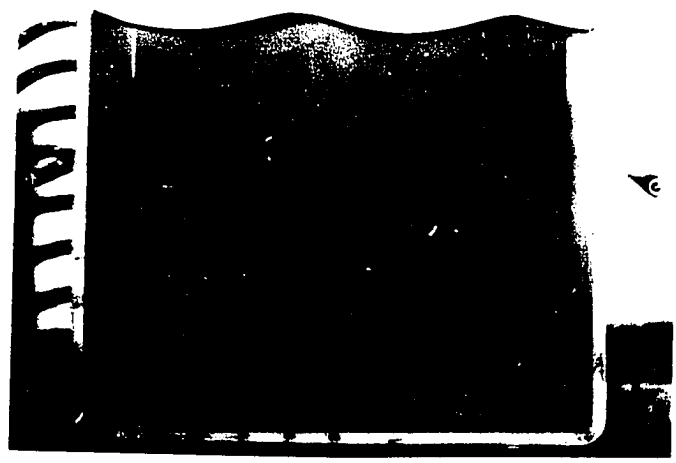

Fig. 25. Motion in the third mode
Frequency 24.9 rad/sec, $\frac{\omega^2 a}{g} = 16$, $h/a = 0.8$

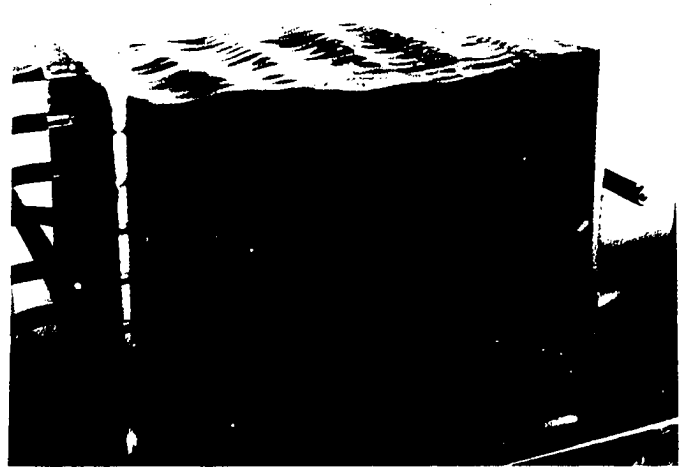

Fig. 26. Motion in the fifth mode
Frequency 33.5 rad/sec, $\frac{\omega^2 a}{g} = 29$, $h/a = 0.8$

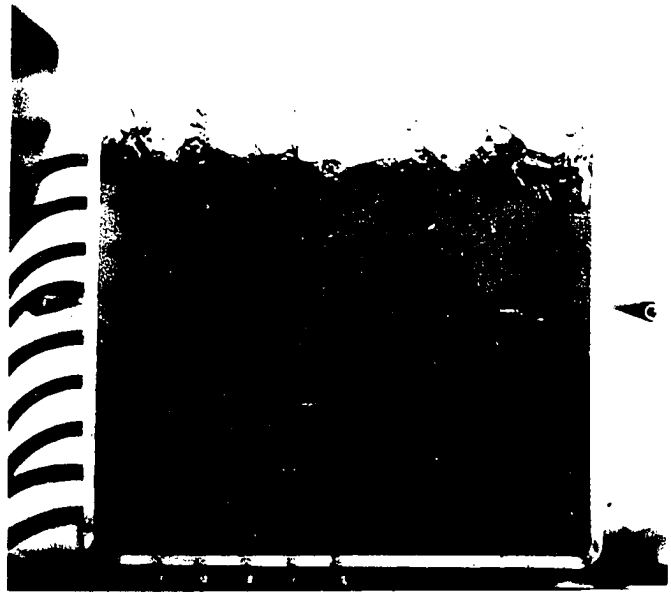

Fig. 27. Splashing mode
Frequency over 44 rad/sec, $\frac{\omega^2 a}{g}$ approximately 50, h/a = 0.8

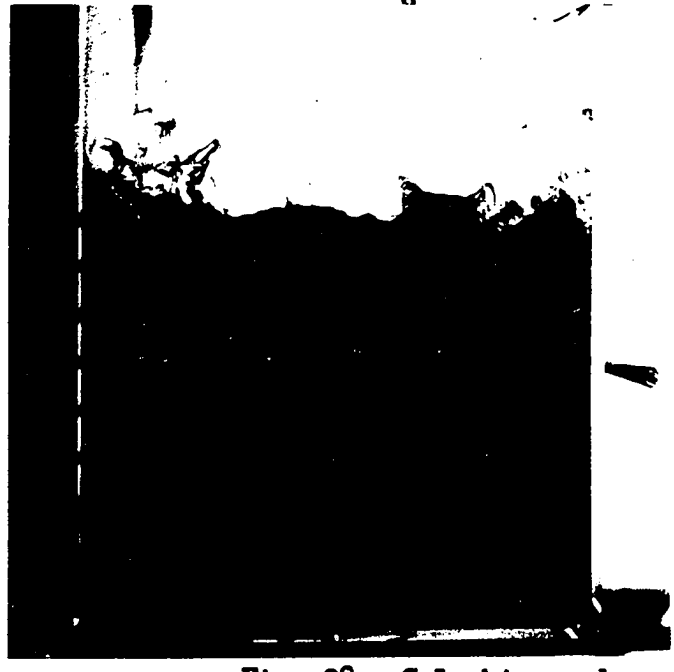

Fig. 28. Splashing mode
Frequency above seventh mode. h/a = 0.8

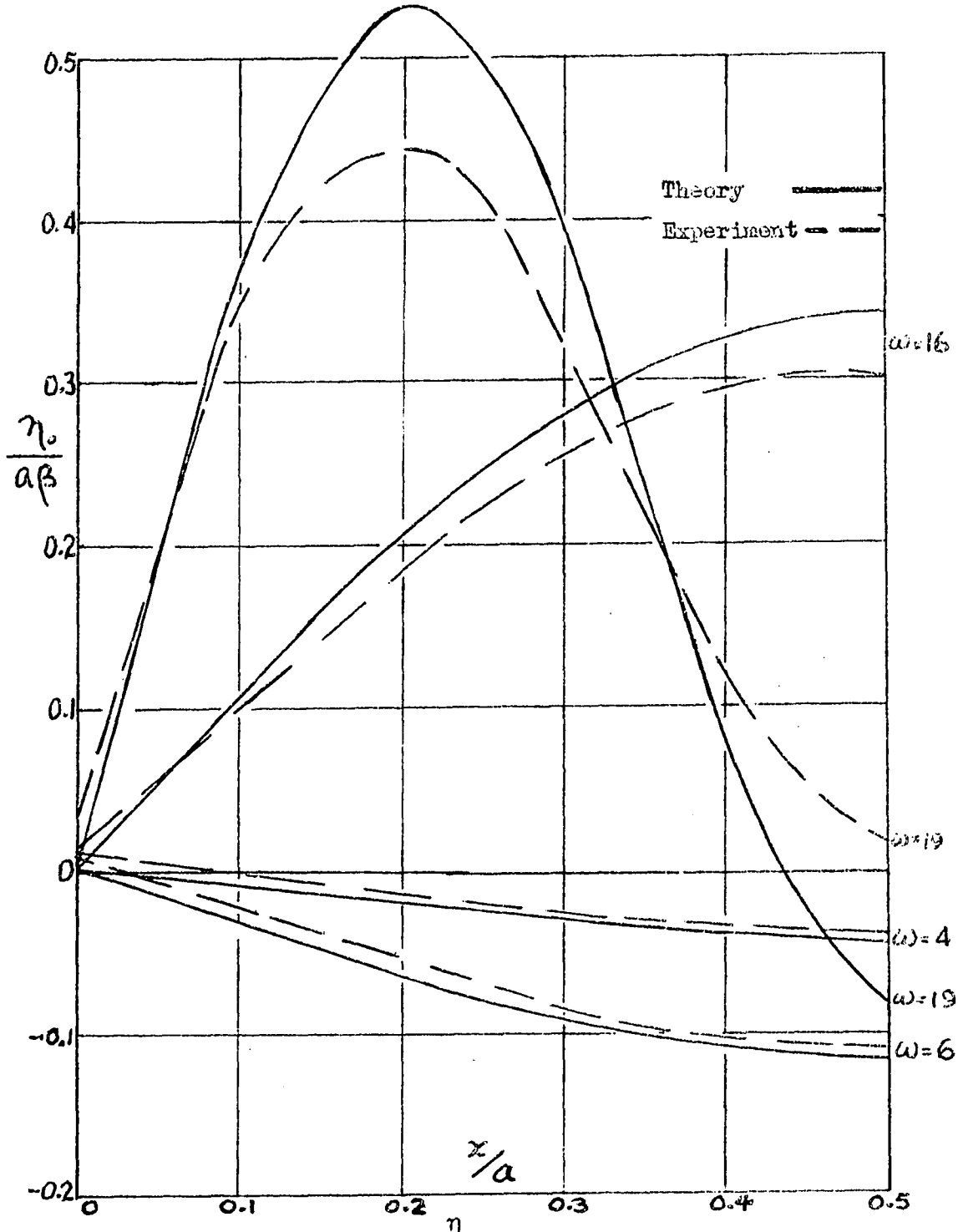

Fig. 29. Wave height $\frac{\eta_0}{a\beta}$ as a function of ω for h/a = 0.4

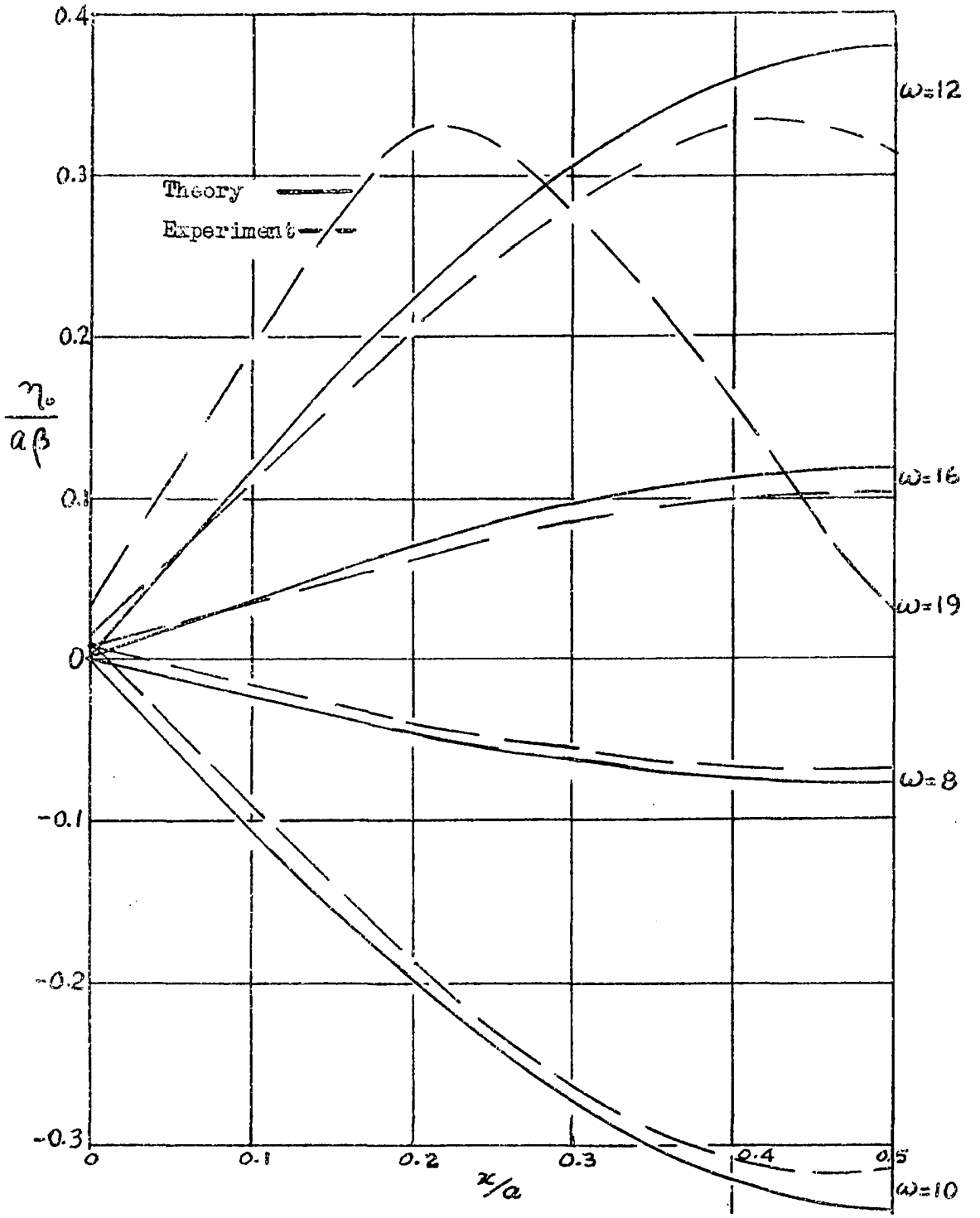

Fig. 30. Wave height $\frac{\eta_o}{a\beta}$ as a function of ω for h/a = 0.8

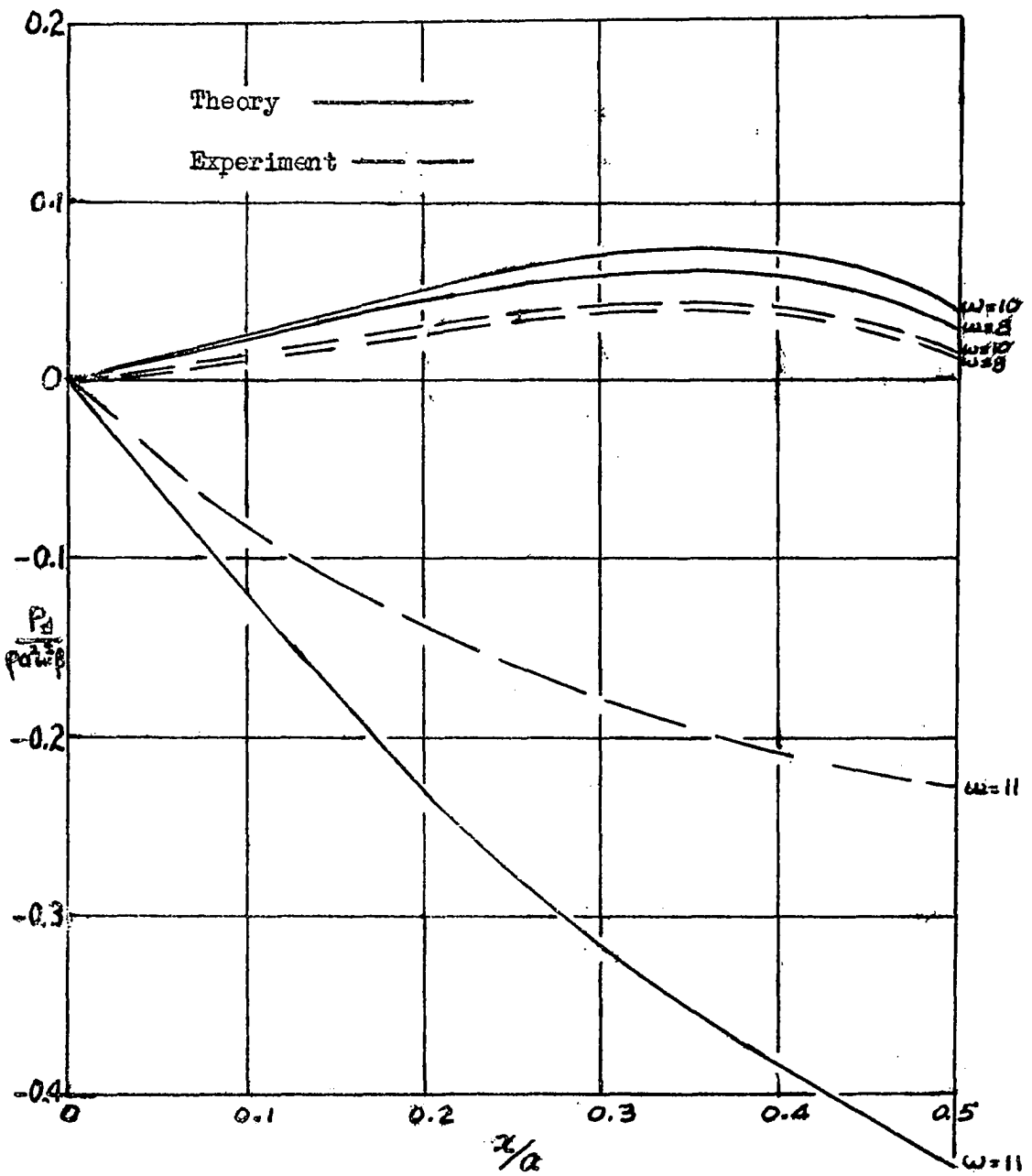

Fig. 31. Pressure $\frac{p_d}{\rho a^2 \omega^2 \beta}$ along bottom as a function of ω for h/a = 0.8

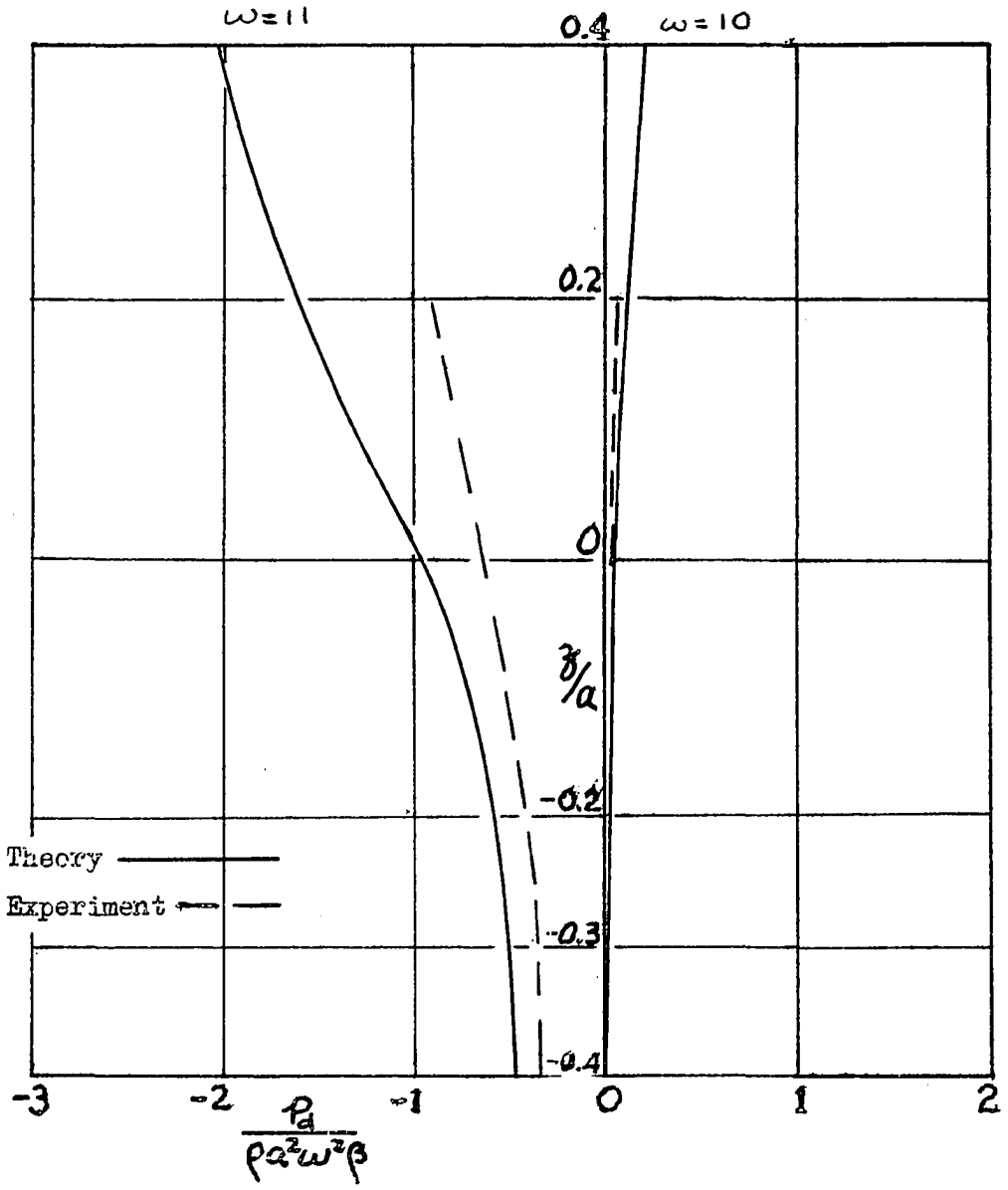

Fig. 32. Pressure $\frac{p_d}{\rho a^2 \omega^2 \beta}$ along end wall as a function of ω for h/a = 0.8

SUMMARY AND CONCLUSIONS

The motion of a fluid in a rectangular pitching vessel was found by using a potential solution. An expression for the natural frequency, surface wave form and pressure along the bottom and end walls was obtained.

Experimental verification of the solution was carried out by taking measurements on a model tank which had a length of ten inches. The tank could be oscillated in a pitching mode at any frequency. Direct measurements and photographs of the wave form confirmed the experimental results. The random method of taking photographs was well justified since most of the pictures taken were of great value in the analysis. Very good agreement was obtained for the natural frequencies and wave shape of the liquid. Pressure readings were more difficult to obtain, but in general substantiate the theory.

It may also be concluded that the viscous damping action in an unbaffled pitching tank is very slight. This confirms the assumption used in the potential solution and is in agreement with results reported for horizontally oscillating vessels containing water or rocket fuel. It was observed that the phase change at a resonant frequency was quite sudden. This result further confirms that the inherent damping during sloshing of a low-viscosity fluid is small.

It is concluded that the natural frequency of fluid oscillation in a rectangular pitching vessel can be accurately predicted. The equation that was developed contains only the odd terms of an equation presented by Lamb (19, p. 440) for the case of standing waves in liquid masses.

The application of similitude to fluid sloshing was considered and the problems involved in model testing were discussed. In low gravitational fields the sloshing motions are affected by surface tension as well as by viscous and inertial forces. A useful dimensionless parameter involving surface tension and gravitational forces was introduced. This parameter determines the degree of control of fluid motion by the surface tension or the gravitational forces.

The critical value defining transition from one form of control to the other was found from results reported for an experiment in a manned space flight in the MA-7 capsule.

SUGGESTIONS FOR FUTURE STUDY

An interesting extension of this research into sloshing would be to investigate the two dimensional form of wave action that occurs under various conditions. Large-amplitude, non-linear motions would also be of interest to investigate. Such motions appeared to be unstable and often developed into two-dimensional wave forms.

A practical extension of this work would be the study of damping of the fluid motion. The objective would be to obtain a rational method of design of a suppression device or system. An important aspect of this would be to develop a theory for scaling of baffle action so that model analysis could be readily used for design.

If fluid damping could be achieved by some form of dynamic action rather than by viscous action alone, then an important advance could be made. It is conceivable that portions of the fluid could be directed by shaped baffles so as to oppose incipient motion. Alternatively a vibration absorber type of device may be developed to suppress a particular mode. Since the fundamental mode is often the only one that creates a problem, such an arrangement should work well.

A very challenging topic would be the development of an electrical or other analogy that would include the free surface or wave effect in a liquid. The several well-known analogies for fluid flow do not account for the possibility of the motion of the surface and so can not be used to study problems with a free surface boundary condition.

LITERATURE CITED

1. Abramson, H. Norman. Amazing motions of liquid propellants. Astronautics 6, No. 3: 35-37, 72, 74. March 1961.

2. Abramson, H. Norman, Martin, R. J. and Ransleben, G. E. Application of similitude theory to the problem of fuel sloshing in rigid tanks. Southwest Research Institute [San Antonio, Texas] Technical Report No. 1. 1958.

3. Abramson, H. Norman and Ransleben, G. E. Simulation of fuel sloshing characteristics in missile tanks by use of small models. Southwest Research Institute [San Antonio, Texas] Technical Report No. 7. 1960.

4. Bauer, H. F. Parametric study of the influence of propellant sloshing on the stability of spacecraft. Journal of the Aerospace Sciences 28: 819-820. 1961.

5. Bauer, H. F. Stability boundaries of liquid-propelled space vehicles with sloshing. American Institute of Aeronautics and Astronautics Journal 1: 1583-1589. 1963.

6. Bauer, H. F. Theory of liquid sloshing in compartmented tanks due to bending excitation. American Institute of Aeronautics and Astronautics Journal 1: 1590-1596. 1963.

7. Berlot, R. R. Production of rotation in a confined liquid through translational motion of the boundaries. Journal of Applied Mechanics 26: 513-516. 1959.

8. Binnie, M. A. Waves in an open oscillating tank. Engineering 151: 224-226. 1941.

9. Case, K. M. and Parkinson, W. C. Damping of surface waves in an incompressible liquid. Journal of Fluid Mechanics 2: 172-184. 1957.

10. Churchill, R. V. Fourier series and boundary value problems. 2nd ed. New York, N.Y., McGraw-Hill Book Company, Inc. c1963.

11. Eulitz, Werner. The sloshing phenomenon and the mechanism of a liquid in motion in an oscillating missile container. U. S. Atomic Energy Commission Report ABMA-R-DS-31 [Army Ballistic Missile Agency, Redstone Arsenal, Alabama]. 1957.

12. Gleghorn, G. J. Present status of the R-W sloshing study program. Mimeographed report. Los Angeles, California. The Ramo-Wooldridge Corporation. 1957.

13. Graham, E. W. The forces produced by fuel oscillation in a rectangular tank. U. S. Atomic Energy Commission Report. SM 13748. [Douglas Aircraft Company, Inc. Santa Monica, California] . 1950.

14. Graham, E. W. and Rodriguez, A. M. The characteristics of fuel motion which affect airplane dynamics. U. S. Atomic Energy Commission Report. SM-14212. [Douglas Aircraft Company, Inc. Santa Monica, California] . 1951.

15. Hoskins, L. M. and Jacobsen, L. S. Water pressure in a tank caused by a simulated earthquake. Seismological Society of America Bulletin 24: 1-32. 1934.

16. Housner, G. W. Dynamic pressures on accelerated fluid containers. Seismological Society of America Bulletin 47: 15-35. 1957.

17. Jacobsen, L. S. Impulsive hydrodynamics of fluid inside a cylindrical tank and of fluid surrounding a cylindrical pier. Seismological Society of America Bulletin 39: 189-204. 1949.

18. Kachigan, K. Forced oscillations of a fluid in a cylindrical tank. Convair, A Division of General Dynamics Corporation [San Diego, California] Report. ZU-7-046. 1955.

19. Lamb, Horace. Hydrodynamics. 6th ed. New York, N.Y., Dover Publications. 1945.

20. Lawrence, H. R., Wang, C. J. and Reddy, R. B. Variational solution of fuel sloshing modes. Jet Propulsion 28: 729-736. 1958.

21. Luskin, H. and Lapin, E. An analytical approach to the fuel sloshing and buffeting problems of aircraft. U. S. Atomic Energy Commission Report. SM-14068. [Douglas Aircraft Company, Inc. Santa Monica, California] . 1951.

22. Merten, K. F. and Stephenson, B. H. Some dynamic effects of fuel motion in simplified model tip tanks on suddenly excited bending oscillations. U. S. National Advisory Committee for Aeronautics Technical Note 2789. 1952.

23. Miles, J. W. An analogy among torsional rigidity, rotating fluid inertia, and self-inductance for an infinite cylinder. Journal of the Aeronautical Sciences 13: 377-380. 1946.

24. Miles, J. W. On the sloshing of liquid in a flexible wall tank. Journal of Applied Mechanics 80: 277-283. 1958.

25. Miles, J. W. Ring damping of free surface oscillations in a circular tank. Journal of Applied Mechanics 80: 274-276. 1958.

26. Murphy, Glenn. Similitude in engineering. New York, N. Y., The Ronald Press Company. c1950.

27. Penny, W. G. and Price, A. T. Finite periodic stationary gravity waves in a perfect fluid. II. Philosophical Transactions Ser. A, 244: 254-284. 1952.

28. Petrash, D. A., Nelson, T. M. and Otto, E. W. Effect of surface energy on the liquid-vapor interface configuration during weightlessness. U. S. National Aeronautics and Space Administration Technical Note D-1582. 1963.

29. Petrash, D. A., Nussle, R. C. and Otto, E. W. Effect of the acceleration disturbances encountered in the MA-7 spacecraft on the liquid vapor interface in a baffled tank during weightlessness. U. S. National Aeronautics and Space Administration Technical Note D-1577. 1963.

30. Petrash, D. A., Zappa, R. F. and Otto, E. W. Experimental study of the effects of weightlessness on the configuration of mercury and alcohol in spherical tanks. U. S. National Aeronautics and Space Administration Technical Note D-1197. 1963.

31. Poisson, S. D. Sur les petites oscillations de l'eau contenue dans un cylindre. Annals de Gergonne 19: 225-240. 1828. Original not available; cited in Lamb, Horace. Hydrodynamics. p. 287. 6th ed. New York, N. Y., Dover Publications. 1945.

32. Rayleigh, [Strutt, John W.] On Waves. Philosophical Magazine Ser. 5, 1: 257-279. 1876.

33. Reese, J. R. and Sewall, J. L. Effective moment of inertia of fluid in offset inclined and swept-wing tanks undergoing pitching oscillations. U. S. National Advisory Committee for Aeronautics Technical Note 3353. 1955.

34. Sandorff, P. E. Principles of design of dynamically similar models for large propellant tanks. U. S. National Aeronautics and Space Administration Technical Note D-99. 1960.

35. Schmitt, A. F. Forced oscillations of a fluid in a cylindrical tank undergoing both translation and rotation. Convair, A Division of General Dynamics Corporation [San Diego, California] Report ZU-7-069. 1956.

36. Schmitt, A. F. Forced oscillations of a fluid in a cylindrical tank oscillating in a carried acceleration field-a correction. Convair, A Division of General Dynamics Corporation [San Diego, California] Report ZU-7-074. 1957.

37. Schy, A. A. A theoretical analysis of the effects of fuel motion on airplane dynamics. U. S. National Advisory Committee for Aeronautics Technical Note 2280. 1951.

38. Smith, C. C. The effects of fuel sloshing on the lateral stability of a free-flying airplane model. U. S. National Advisory Committee for Aeronautics Research Memorandum L8C16. 1948.

39. Stofan, A. J. and Sumner, I. E. Experimental investigation of the slosh-damping effectiveness of positive-expulsion bags and diaphragms in spherical tanks. U. S. National Aeronautics and Space Administration Technical Note D-1712. 1963.

40. Stoker, J. J. Water waves. New York, N. Y., Interscience Publishers, Inc. 1957.

41. Streeter, V. L. Fluid dynamics. New York, N. Y., McGraw-Hill Book Company, Inc. 1948.

42. Sumner, I. E. Preliminary experimental investigation of frequencies and forces resulting from liquid sloshing in toroidal tanks. U. S. National Aeronautics and Space Administration Technical Note D-1709. 1963.

43. Taylor, Geoffrey. An experimental study of standing waves. Royal Society of London Proceedings, Ser. A, 218: 44-59. 1953.

44. Werner, P. W. and Sundquist, K. J. On hydrodynamic earthquake effects. American Geophysical Union Transactions 30: 636-657. 1949.

45. Westergaard, H. M. Water pressures on dams during earthquakes. American Society of Civil Engineers Transactions 98: 418-433. 1933.

46. Widmayer, E. W. and Reese, J. R. Moment of inertia and damping of fluid in tanks undergoing pitching oscillations. U. S. National Advisory Committee for Aeronautics Research Memorandum L53E01a. 1953.

47. Zangar, C. N. Hydrodynamic pressures on dams due to horizontal earthquakes. Society for Experimental Stress Analysis Proceedings 10: 93-102. 1953.

ACKNOWLEDGMENTS

The author would like to express his sincere gratitude to Dr. Glenn Murphy, Head of the Department of Nuclear Engineering, for his guidance, encouragement and criticism during the preparation of this thesis.

This study was conducted as part of a graduate program in the Department of Theoretical and Applied Mechanics with minors in Mathematics and Aerospace Engineering. The author wishes to extend his appreciation to all those members of the Iowa State University staff in these departments who have offered suggestions and assistance during his program.